Chymotrypsin activity signals to intestinal epithelium by protease-activated receptor-dependent mechanisms

Simon Guignard, Mahmoud Saifeddine, Koichiro Mihara, Majid Motahhary, Magali Savignac, Laura Guiraud, David Sagnat, Mireille Sebbag, Sokchea Khou, Corinne Rolland, et al.

RESEARCH ARTICLE

BJP · BRITISH PHARMACOLOGICAL SOCIETY

Chymotrypsin activity signals to intestinal epithelium by protease-activated receptor-dependent mechanisms

Simon Guignard[1] | Mahmoud Saifeddine[2,3] | Koichiro Mihara[2,3] |
Majid Motahhary[2,3] | Magali Savignac[4] | Laura Guiraud[1] | David Sagnat[1] |
Mireille Sebbag[1] | Sokchea Khou[1] | Corinne Rolland[1] | Anissa Edir[1] |
Barbara Bournet[5] | Louis Buscail[5] | Etienne Buscail[1,6] | Laurent Alric[7] |
Caroline Camare[8,9] | Mouna Ambli[1] | Nathalie Vergnolle[1,2] |
Morley D. Hollenberg[2,3] | Céline Deraison[1] | Chrystelle Bonnart[1]

[1]IRSD, University of Toulouse, INSERM, INRAE, ENVT, Université Toulouse III—Paul Sabatier (UPS), Toulouse, France

[2]Department of Physiology and Pharmacology, University of Calgary Cumming School of Medicine, Calgary, Alberta, Canada

[3]Department of Medicine, University of Calgary Cumming School of Medicine, Calgary, Alberta, Canada

[4]Toulouse Institute for Infectious and Inflammatory Diseases (Infinity) INSERM UMR1291—Centre National de la Recherche Scientifique UMR5051, Université Toulouse III—Paul Sabatier (UPS), Toulouse, France

[5]Department of Gastroenterology, Toulouse University Hospital, Toulouse, France

[6]Department of Digestive Surgery, Toulouse University Hospital, Toulouse, France

[7]Department of Internal Medicine and Digestive Diseases, Rangueil, Toulouse III University Hospital, University of Toulouse, Toulouse, France

[8]Department of Clinical Biochemistry, Toulouse University Hospital, Toulouse, France

[9]University of Toulouse, UMR1297, INSERM/Université Toulouse III—Paul Sabatier (UPS), Toulouse, France

Correspondence
Nathalie Vergnolle, Institut de Recherche en Santé Digestive (IRSD), INSERM UMR1220, Purpan Hospital, CS60039, 31024 Toulouse Cedex 03, France.
Email: nathalie.vergnolle@inserm.fr

Abstract

Background and Purpose: Chymotrypsin is a pancreatic protease secreted into the lumen of the small intestine to digest food proteins. We hypothesized that chymotrypsin activity may be found close to epithelial cells and that chymotrypsin signals to them via protease-activated receptors (PARs). We deciphered molecular pharmacological mechanisms and gene expression regulation for chymotrypsin signalling in intestinal epithelial cells.

Experimental Approach: The presence and activity of chymotrypsin were evaluated by Western blot and enzymatic activity tests in the luminal and mucosal compartments of murine and human gut samples. The ability of chymotrypsin to cleave the extracellular domain of PAR1 or PAR2 was assessed using cell lines expressing N-terminally tagged receptors. The cleavage site of chymotrypsin on PAR1 and PAR2 was determined by HPLC–MS analysis. The chymotrypsin signalling mechanism was

Abbreviations: BAPTA-AM, 1,2-bis(2-aminophenoxy)ethane-N,N,N′,N′-tetraacetic acid tetrakis(acetoxymethyl ester); BTP2, N-[4-[3,5-bis(trifluoromethyl)-1H-pyrazol-1-yl]phenyl]-4-methyl-1,2,3-thiadiazole-5-carboxamide; CRACs, Ca^{2+} release-activated Ca^{2+} channels; CTRB, chymotrypsin B; ER, endoplasmic reticulum; IECs, intestinal epithelial cells; NEAA, non-essential amino acid solution; nLuc, nanoluciferase; PARs, protease-activated receptors; P-ERK, phosphorylated extracellular signal-regulated kinase; PTX, pertussis toxin; SOCE, store-operated calcium entry; TLs, tethered ligands; TLCK, Nα-tosyl-L-lysine chloromethyl ketone hydrochloride.

investigated in CMT93 intestinal epithelial cells by calcium mobilization assays and Western blot analyses of (ERK1/2) phosphorylation. The transcriptional consequences of chymotrypsin signalling were analysed on colonic organoids.

Key Results: We found that chymotrypsin was present and active in the vicinity of the colonic epithelium. Molecular pharmacological studies have shown that chymotrypsin cleaves both PAR1 and PAR2 receptors. Chymotrypsin activated calcium and ERK1/2 signalling pathways through PAR2, and this pathway promoted interleukin-10 (IL-10) up-regulation in colonic organoids. In contrast, chymotrypsin disarmed PAR1, preventing further activation by its canonical agonist, thrombin.

Conclusion and Implications: Our results highlight the ability of chymotrypsin to signal to intestinal epithelial cells via PARs, which may have important physiological consequences in gut homeostasis.

KEYWORDS
calcium signalling, chymotrypsin, intestinal epithelium, MAPK, organoids, PAR1, PAR2

1 | INTRODUCTION

The intestinal epithelium is constantly exposed to luminal material such as the microbiota, its metabolites, diet residues and host secretion products, including pancreatic juice. The latter component contains a large amount of **proteases** (trypsins, chymotrypsins and elastases) that have an essential role in the digestion of dietary proteins (Pandol, 2010). Although historically considered only as degradative enzymes, proteases are now viewed as true signalling mediators, thanks to their ability to interact with protease-activated receptors (**PARs**). PARs are G protein-coupled receptors (GPCRs) whose activation regulates many physiological and pathophysiological processes, particularly in the gut (Adams et al., 2011; Alexander, Christopoulos, et al., 2023; Caminero et al., 2019; Peach et al., 2023; Sebert et al., 2019; Vergnolle, 2005, 2016).

Unlike other GPCRs, the ligands for PARs are located within the extracellular N-terminus of the receptors themselves and are hence called tethered ligands (TLs). The proteolytic cleavage of PARs at defined canonical sites situated at the N-terminal side of the TLs enables its binding to the second extracellular loop of the cleaved receptor (Ramachandran et al., 2012). This binding induces conformational changes in the receptor that trigger downstream intracellular signals. However, while some proteases activate PARs by this mechanism, others have the ability to hinder PAR activation by cleaving their extracellular part at sites located downstream of the TLs. This disarming cleavage makes them unusable for further proteolytic activation (Dulon et al., 2003; Holzhausen et al., 2006; Mihara et al., 2013). Nevertheless, some cleavages that sever the TL sequence downstream from the receptor's canonical activation site can also cause distinct signalling, a phenomenon called biased signalling (Hollenberg et al., 2014; Ramachandran et al., 2011). Synthetic agonist peptides mimicking the TLs can also directly activate either uncleaved or N-terminally cleaved receptors, representing useful tools to study the pharmacology of PARs.

What is already known

- Chymotrypsin is a pancreatic serine protease which breaks down food proteins in the gut lumen.
- PAR1 and PAR2 are protease-activated receptors expressed by intestinal epithelial cells.

What does this study add

- Active chymotrypsin regulates signalling in epithelial cells through PAR2 activation and PAR1 disarming.
- Chymotrypsin regulates the transcriptional profile of colonic organoids via PAR2-dependent and PAR2-independent mechanisms.

What is the clinical significance

- This novel signalling function of chymotrypsin opens new treatments for pathologies involving PAR1 and PAR2.
- The PAR1 disarming effect of chymotrypsin could impact the therapeutic control of platelet activation.

Once activated, PARs can mediate a broad diversity of intracellular signals depending on the TL sequence unmasked by the cleaving protease and the ability of the receptor to interact with distinct Gα protein subtypes (Ramachandran et al., 2012). Depending on the α subunit involved, distinct signalling pathways have been described downstream of PAR activation like Ca^{2+} mobilization, mitogen-activated protein

kinase (MAPK) phosphorylation, cAMP inhibition or Rho-associated kinase activation (Adams et al., 2011; Ramachandran et al., 2016, 2012).

Four versions of PARs (PAR1–PAR4) have been described, which are widely expressed throughout the body. Literature reports that PAR1 and PAR2 are the two main PARs expressed by the gut epithelium. PAR2 is strongly detected in the gastrointestinal (GI) tract of humans and rodents, including in the stomach, the small intestine and the colon (Bohm et al., 1996; Kong et al., 1997; Nystedt et al., 1994; Nystedt, Emilsson, et al., 1995; Nystedt, Larsson, et al., 1995). Among the numerous cell types expressing this receptor, a clear immunolabelling of the epithelial compartment was reported in human and murine colon samples, especially at the apical side (Cenac et al., 2002; Cuffe et al., 2002; D'Andrea et al., 1998; Nasri et al., 2016). Lau et al. (2011) reported the existence of distinct apical and basolateral membrane pools of PAR2 in Caco2-BBe cells and in the mouse ileum. Regarding PAR1, while Darmoul et al. (2003) first indicated that this receptor is largely confined to cancerous colonic tissues and tumour-derived cell lines, many other publications suggest an expression of functional PAR1 in non-transformed intestinal epithelial cells (IECs) (Buresi et al., 2001; Reinhardt et al., 2012; Sebert et al., 2018). Activation of PAR1 by thrombin, its canonical protease agonist, promotes chloride secretion in non-transformed SCBN epithelial cells (Buresi et al., 2001). Moreover, apical stimulation of these cells with PAR1 agonists has also been reported to promote apoptosis (Chin et al., 2003), showing a functional PAR1 pool at membranes facing the lumen. Finally, both PAR1 and PAR2 have been shown to induce effects in vivo when their agonists are administered intrarectally, likely involving direct activation of apical pools of receptors (Cenac et al., 2002; Chin et al., 2003; Motta, Palese, et al., 2021; Nguyen et al., 2003).

Chymotrypsin is a major serine protease produced by the pancreas and secreted into the gut lumen. Its primary and essential function is to digest dietary proteins into small peptides that can then be absorbed throughout the body. It is well established that pancreatic chymotrypsin is activated in the duodenum, the intestinal segment where its proteolytic activity is highest (Borgstrom et al., 1957; Goldberg et al., 1969). Chymotrypsin activity then progressively decreases along the small intestine but is still elevated in the ileum. Of importance, active chymotrypsin has been detected at the surface of the small intestinal mucosa, highlighting a direct contact between this enzyme and the epithelial cells (Goldberg et al., 1968). In addition, chymotrypsin activity is still detectable in human faeces and was proposed as a marker for pancreatic exocrine function (Remtulla et al., 1986; Smith et al., 1971). Due to the presence of a thick mucus layer in the large intestine, whether chymotrypsin activity might be found in the vicinity of the colonic epithelium is still an open question. As well, its action on PARs and its potential effects on the host intestinal epithelium have never been addressed before.

In this study, we report the presence of active chymotrypsin neighbouring the colonic mucosal surface. In addition, we identified that chymotrypsin is able to cleave PAR2 and activate downstream calcium and extracellular signal-regulated kinase 1/2 (ERK1/2) signalling pathways in CMT93 colonic epithelial cells. Using primary colonic epithelial cell 3D cultures (organoids), our data show that this pathway up-regulated the gene expression of interleukin-10 (IL-10), an anti-inflammatory cytokine. Furthermore, our results show that chymotrypsin disarms PAR1, thereby preventing further activation of the receptor by its canonical agonist, thrombin. These results shed new light on the function of chymotrypsin in the gut, which is able to regulate PAR-dependent signalling pathways.

2 | METHODS

2.1 | Reagents

All reagents were prepared according to the recommendations of the manufacturer. Chymotrypsin purified from bovine pancreas and treated with $N\alpha$-tosyl-L-lysine chloromethyl ketone hydrochloride (TLCK, a trypsin inhibitor) was prepared as a stock solution at 1000 U·ml^{-1} in 1-mM HCl–2-mM CaCl$_2$ (Sigma-Aldrich, St. Louis, MI, USA, reference C3142). For some experiments, inactivated chymotrypsin was prepared by heating for 1 h at 95°C. Trypsin purified from bovine pancreas and devoid of chymotrypsin activity by tosyl phenylalanyl chloromethyl ketone (TPCK) treatment (T1426), human plasma thrombin (T6884), the chymotrypsin inhibitor chymostatin (C7268), the cysteine protease inhibitor E-64 (E3132), the trypsin-like inhibitor TLCK (T7254), the aspartic protease inhibitor pepstatin A (P5318) and the serine protease inhibitor AEBSF (A8456) were all purchased from Sigma-Aldrich. The elastase inhibitor elastatinal (sc-201272) was from Santa Cruz Biotechnology, Dallas, TX, USA. The fluorogenic chymotrypsin substrate, Suc–Ala–Ala–Pro–Phe–aminomethyl coumarin (AMC), was provided by Bachem (4012873).

The C-terminally amidated PAR1 agonist peptide TFLLR-NH$_2$ and PAR2 agonist peptide SLIGRL-NH$_2$ were obtained from the GenScript Company, Piscataway, NJ, USA (20354 and RP19975, respectively). The PAR2 agonist peptide, 2-furoyl-LIGRLO-NH$_2$ (2fLI), and the PAR1 and PAR2 N-terminal peptides used for chymotryptic cleavage experiments (NATLDPRSFLLRNPNDKYE-NH$_2$ and TNRSSKGRSLIGKVDGT SHVTGKGVT-NH$_2$, respectively) were prepared by the peptide synthesis facility of the University of Calgary, Canada (>95% purity by high-performance liquid chromatography [HPLC]). The PAR1 antagonist, F16357, was from Pierre Fabre Medicament (Toulouse, France). The PAR2 antagonist I-191 was purchased from Axon Medchem (Reston, VA, USA, 3043). 1,2-Bis(2-aminophenoxy)ethane-N,N,N',N'-tetraacetic acid tetrakis(acetoxymethyl ester) (BAPTA-AM), a calcium chelator, was purchased at Abcam (Cambridge, UK, ab120503). N-{4-[3,5-Bis(trifluoromethyl)-1H-pyrazol-1-yl]phenyl}-4-methyl-1,2,3-thiadiazole-5-carboxamide (BTP2) was from Merck Millipore (Burlington, MA, USA, 203890), and ethylene glycol-bis(β-aminoethyl ether)-N,N,N',N'-tetraacetic acid (EGTA) was purchased from Sigma-Aldrich (E3889). The following inhibitors were used for signalling experiments: YM-254890 (G$_q$ inhibitor, AdipoGen Life Sciences, San Diego, CA, USA, AG-CN2-0509), pertussis toxin (PTX) (G$_{i/o}$ inhibitor, Sigma-

Aldrich, 516560) and Y-27632 (Rho-dependent $G_{12/13}$ inhibitor, Sigma-Aldrich, Y0503).

2.2 | Human samples

All human biological samples were obtained from informed consenting patients treated at Toulouse Hospital (Centre Hospitalier Universitaire de Toulouse) after receiving ethics committee approval under Protocol Numbers CAPITOL RC31/21/038, COLIC DC-2015-2443, NCT05251415 and BACAP NCT02818829 (Canivet et al., 2018) approved by the relevant Comité de Protection des Personnes (CPP Sud-Ouest et Outre-Mer I et II).

Human colonic mucus was obtained from macroscopically healthy zones, taken during surgical resections in patients with colorectal cancer or inflammatory bowel diseases. Upon reception, tissues were mechanically cleaned of any residual faecal material, and the surface of the mucosa was gently scraped using a cell scraper to harvest the mucus. The viscous material obtained was homogenized for 30 s using a Benchmark D1000 homogenizer in a buffer containing 100-mM Tris–HCl (pH 8), 1-mM $CaCl_2$ and 1-mM CHAPS. The obtained mucus extract was then clarified by centrifugation (10 min—2300 g at 4°C) and tested for the presence of chymotrypsin by proteolytic assays and Western blot analyses. The Immuno-related procedures used comply with the recommendations made by the British Journal of Pharmacology (Alexander et al., 2018).

Human colonic mucosal biopsies were obtained during colonoscopies in patients undergoing colorectal cancer screening. The tissue was placed in 300 μl of the buffer described above and homogenized in tubes containing ceramic beads (MP Biomedicals, Irvine, CA, USA, 6913500) using a 3D bead-beating tissue homogenizer (Precellys, Bertin Technologies, Montigny-le-Bretonneux) for 20 s at 6800 r.p.m. and then centrifuged for 10 min at 2300 g. The obtained extract was then evaluated in Western blot to assess the presence of chymotrypsin.

Human stools were obtained from healthy donors and, upon receipt, divided into two differentially processed portions. Regarding batches dedicated to Western blot analysis, 30 mg was placed in 1.5 ml of phosphate-buffered saline (PBS) supplemented with 0.01% NP-40 lysis buffer, 0.1% sodium dodecyl sulfate (SDS), 12-mM deoxycholic acid and a protease inhibitor cocktail (Roche, Basel, Switzerland, 11836170001), homogenized in tubes containing ceramic beads using a 3D bead-beating tissue homogenizer for 2×30 s at 5000 r.p.m. and then centrifuged for 10 min at 1000 g. The resulting supernatants were mixed with Laemmli buffer (62.5-mM Tris–HCl [pH 6.8], 2% SDS, 10% glycerol, 0.01-mg·ml^{-1} bromophenol blue and 5% β-mercaptoethanol) after protein quantification by the bicinchoninic acid (BCA) assay method. For the assay of proteolytic activity, 30 mg of faecal samples was also placed in tubes containing ceramic beads and 1.5 ml of protease activity assay buffer (100-mM Tris–HCl [pH 8], 1-mM $CaCl_2$ and 1-mM CHAPS). Samples were then homogenized for 2×30 s at 5000 r.p.m. with a Precellys tissue homogenizer and finally clarified by centrifugation (10 min—2300 g at 4°C).

Human pancreatic tissue was obtained from a surgical resection during the Whipple procedure. The tissue was homogenized in TRI Reagent® (Molecular Research Center, Cincinnati, OH, USA, TR 118) using a Benchmark D1000 homogenizer. After the addition of 200-μl chloroform, centrifugation at 12,000 g for 15 min at 4°C and removal of the aqueous phase, protein precipitation was performed on the remaining organic phase by mixing it with 1 volume of isopropanol. After centrifugation at 2000 g for 20 min at 4°C, the protein pellet was washed twice with 50% ethanol and resuspended in 2% SDS.

2.3 | Mouse samples

Animal studies are reported in compliance with the ARRIVE guidelines (Percie du Sert et al., 2020) and with the recommendations made by the British Journal of Pharmacology (Lilley et al., 2020). C57BL/6J mice were used in this study. They were initially purchased from Janvier Laboratory (Le Genest-Saint-Isle, France) and bred at the US006/INSERM animal facility (Toulouse, France) in ventilated cages (five mice maximum per cage) in a specific pathogen-free area. They had free access to food and water and were maintained on 12-h light/dark cycles. They were moved and acclimated to the local animal facility at least 1 week before death at 7–12 weeks of age. This was done by cervical dislocation after the collection of fresh faeces, which were immediately frozen in liquid nitrogen. From these faecal samples, native protein extracts were prepared as follows and used for Western blot and proteolytic assays. Frozen murine stools were homogenized twice in 1.5 ml of radioimmunoprecipitation assay (RIPA) buffer (1% NP-40, 0.5% deoxycholic acid and 0.1% SDS) for 30 s at 4500 r.p.m. using a Precellys tissue homogenizer followed by the removal of insoluble material by a 10-min centrifugation at 2300 g and 4°C.

Murine pancreas was resected and prepared as described for human pancreas. Lung protein extracts were prepared by homogenization in lysis buffer (Pierce IP Lysis Buffer, Thermo Fisher Scientific, Waltham, MA, USA) using the 3D bead-beating tissue homogenizer for 2×30 s at 6800 r.p.m., followed by the removal of solid residual material by centrifugation at 13,000 g for 5 min at 4°C.

The colon was resected, and mucosal scrapings were performed using different strategies. In order to preserve the mucosa-associated material for proteolytic activity and Western blot assays, the colon was opened longitudinally, the residual faecal material was mechanically removed and the mucosa was scraped using a microscopy slide. In contrast, for some Western blot experiments, the luminal surface of the colon was pre-washed with 15 ml of PBS before opening, in order to remove any mucosa-associated material and retain only the host mucosal cells. This washed mucosa was then scrapped as described above. All mucosal scrapings were then homogenized for 2×15 s at 4500 r.p.m. using a Precellys tissue homogenizer in lysis buffer supplemented with a cocktail of protease inhibitors (100-μM E-64, 100-μM pepstatin, 135-μM TLCK and 100-μM elastatinal) targeting a wide spectrum of protease activities

except those belonging to the chymotrypsin family. All samples were then cleared of residual solid particles by centrifugation (5 min— 13,000 g at 4°C) before analysis.

2.4 | Preparation of PAR2-null HEK293 and CMT93 cells

$PAR2^{-/-}$ human embryonic kidney cells (HEK293) were derived from the HEK293 cell line (RRID:CVCL_0045) constitutively expressing functional PAR1 and PAR2 (Kawabata et al., 1999), using a CRISPR approach similar to that described for the generation of $PAR1^{-/-}$ HEK293 cells in Mihara et al. (2016). The three target sequences for CRISPR knockout of PAR2 were derived from the human PAR2/F2RL1 genomic sequence (HGLibA_15864: GTCT GCTTCACGACATACAA; HGLibA_15865: GGAACCAGTAGATCCTC-TAA; and HGLibA_15866: CCCCAGCAGCCACGCCGCGC). Cells were transfected with Lipofectamine LTX (Thermo Fisher Scientific) and maintained in the presence of $5-\mu g \cdot ml^{-1}$ puromycin to select knockout cells.

Murine colonic epithelial CMT93 cells deficient in PAR2 ($PAR2^{-/-}$) were generated using Crispr/Cas9 technology as described in Nasri et al. (2016). Briefly, CMT93 cells were electroporated with the mPAR2 Crispr/Cas9 plasmid (sc-420265, Santa Cruz Biotechnology). Transfected cells were sorted by flow cytometry to isolate green fluorescent protein (GFP)-positive cells from which clones were isolated and amplified.

Both HEK and CMT93 $PAR2^{-/-}$ cells were validated by checking the loss of calcium mobilization effect in an assay using PAR2 agonist peptides (Figure S1A,B).

2.5 | Culture of human primary organoids and treatments

Human colonic tissues were obtained from resections taken from macroscopically intact areas of patients suffering from colorectal cancers. Epithelial cell crypts were isolated from colonic sample tissues and cultured as described in Sebert et al. (2018). Briefly, the crypts were resuspended in a jellifying basement membrane matrix (Matrigel©, Corning, NY, USA, 354277) at 2 crypts/μl and seeded as 25-μL matrix domes (1 dome per well) in 48-well culture plates (Greiner Bio-One, Kremsmünster, Austria). After matrix gelation, 250 μl of culture medium was added to each well (see Table S1). The medium was changed every 2 days. On Day 4, $0.5-U \cdot ml^{-1}$ chymotrypsin or its vehicle (buffer containing 1-mM HCl and 2-mM $CaCl_2$) was added to the culture medium of organoids. The treatment was renewed every 2 days until Day 8, inclusive. In addition, I-191 (10 μM), a PAR2 antagonist, or its vehicle (0.05% dimethyl sulfoxide [DMSO]) was added 45 min before chymotrypsin treatment. Unfortunately, the highest concentrations of chymotrypsin could not be used because they degraded the Matrigel© matrix. On Day 10, the medium was removed and the Matrigel© was dissolved by

incubation with 250 μl of PBS supplemented with 5-mM ethylenediaminetetraacetic acid (EDTA) for 10 min at 4°C. Organoids were centrifuged at 400 g for 3 min, and the pellet was lysed in TRI Reagent®.

2.6 | Reverse transcription and quantitative polymerase chain reaction (RT-qPCR) analyses

Total RNAs were extracted from the organoid samples using the Direct-zol DNA/RNA Miniprep kit (Ozyme, R2080), following the manufacturer's instructions. Reverse transcription was realized using a range of 500- to 1500-μg RNA with the SuperScript™ III First-Strand Synthesis System (Invitrogen, Carlsbad, CA, USA, 18080051). For quantitative polymerase chain reaction (qPCR) experiments, 15 ng of cDNA was mixed with 600-nM primers and 5-μl Takyon NO ROX SYBR 2X MasterMix blue dTTP (Eurogentec) in a final volume of 10 μl. qPCR was performed using a LightCycler® 480 System (Roche) following an initial denaturation at 95°C for 5 min followed by 45 cycles of (15 s at 95°C–20 s at 60°C–20 s at 72°C). Cycle threshold (Ct) was extracted from the graphs using the LightCycler® 480 software. Relative ratios were calculated following the $2^{-\Delta\Delta CT}$ method (Livak & Schmittgen, 2001), using Hprt as a housekeeping gene. All primer sequences and the function of the target genes are indicated in Table S2.

2.7 | Cloning and transfection of Chinese hamster ovary (CHO) cells

Engineered receptors with a nanoluciferase (nLuc) inserted at the N-terminus of human PAR1 or PAR2 were created to monitor the extracellular cleavage of PAR molecules. These receptors also contained an eYFP inserted at the C-terminus of PAR1 or PAR2. The details of the construction strategy are as follows.

The pCDNA3.1–hPAR1 and pcDNA3.1–hPAR2 were obtained from the cDNA Recourse Center (Bloomsburg, PA). The nLuc containing vector (pNL1.1) was a gift from Promega (Madison, WI, USA). The stop codon of hPAR1 in pcDNA3.1 was replaced by a tyrosine-encoding codon by site-directed mutagenesis, and the coding sequence of eYFP (flanked by XhoI and XbaI restriction sites) was cloned downstream and in frame of the PAR1 sequence, giving a pcDNA–PAR1–eYFP vector. Restriction sites of BspEI and BamHI were then added by site-directed mutagenesis at S31 of PAR1, allowing the insertion of an nLuc polymerase chain reaction (PCR) fragment upstream of the PAR1–eYFP cDNA. The resulting vector was named pcDNA–nLuc–PAR1–eYFP. For PAR2, similar constructs were generated using this strategy (nLuc inserted at the Q27 site of hPAR2). CHO-K1 cells were transfected with the nLuc–hPAR1/2–eYFP pCDNA plasmids using the GeneJuice® transfection reagent kit (Sigma-Aldrich, 70967), according to the manufacturer's instructions. The transfected cells were selected with G418 at $1.5 \text{ mg} \cdot ml^{-1}$ (Sigma-Aldrich, A1720) for 1 week.

For other experiments, site-directed mutagenesis was performed on the pcDNA3.1–hPAR2 to create a R^{36}/G mutant of hPAR2, using the QuikChange Lightning Multi Site-Directed Mutagenesis Kit (Agilent Technologies, Mississauga, ON, Canada). This plasmid was transfected in double-deficient PAR1$^{-/-}$ and PAR2$^{-/-}$ HEK cells.

2.8 | Cell culture

All cell lines were maintained at 37°C and 5% CO_2, and the medium was changed every 2 days. Cells were subcultured when they reached 90% confluence.

CMT93 cells (ATCC-CCL-223, RRID:CVCL_1986) were grown in Dulbecco's modified Eagle's medium (DMEM, Gibco) supplemented with 100-U·ml^{-1} penicillin/streptomycin, 10% fetal calf serum (FCS) and 1% non-essential amino acid solution (NEAA). PAR2$^{-/-}$ CMT93 cells were grown in a similar medium supplemented with 0.7-mg·ml^{-1} G418.

CHO cells (RRID:CVCL_0213) stably transfected with nLuc–PAR1/2–YFP were cultured in Ham's F-12 (Gibco) supplemented with 10% FCS and 1% NEAA, in the presence of G418 at 0.7 mg·ml^{-1}.

All HEK293 cells (wild-type [WT] and mutant) were routinely maintained in DMEM supplemented with 1-mM sodium pyruvate, 10% FCS and 2.5 μg·ml^{-1} of Plasmocin (InvivoGen, San Diego, CA, USA). Sub-culturing was performed without trypsin by cell dissociation using enzyme-free buffer (PBS [pH 7.4], containing 1-mM EDTA). The CRISPR-derived PAR2$^{-/-}$ HEK cells were maintained in regular medium containing 5-μg·ml^{-1} puromycin to preserve their knockout status.

2.9 | Determination of PAR1 and PAR2 cleavage sites by chymotrypsin

Peptides corresponding to a region of the N-terminal extracellular domain of human PAR1 and PAR2 containing the TL sequence were produced at the Faculty of Peptide Synthesis at the University of Calgary (hPAR1: NATLDPRSFLLRNPNDKYE; hPAR2: N-acetyl-GT NRSSKGRSLIGKVDGTSHVTGKGVT-amide [TL-activating sequences are underlined]). Peptides (100 μM final) were incubated with 5-U·ml^{-1} chymotrypsin for 30 min at 37°C. Reactions were stopped by adding 1 volume of 50% acetonitrile and 0.1% trifluoroacetic acid to water. Samples were fractionated by reversed-phase HPLC, and eluted peptides were analysed by mass spectrometry as outlined previously (Oikonomopoulou et al., 2006).

2.10 | Detection of ERK1/2 activation

For all experiments, WT or PAR2$^{-/-}$ CMT93 cells were plated at 250,000 cells per well in six-well plates in culture medium. The day after, cells were washed three times in PBS and maintained in Hank's balanced salt solution (HBSS, Gibco, 14025092) for 16 h.

For the study of PAR2-dependent signalling, cells were then stimulated with different concentrations of chymotrypsin for 10 min. At the end of incubation, cells were placed on ice, washed once in PBS and lysed in the IP Lysis Buffer (Thermo Fisher Scientific) supplemented with a protease inhibitor (cOmplete™, Roche) and a phosphatase inhibitor cocktail (P5726, Sigma-Aldrich). Protein lysates were centrifuged at 1000 g for 5 min at 4°C to eliminate insoluble material. These extracts were diluted in LDS NuPAGE buffer (Invitrogen) supplemented with 5% β-mercaptoethanol and used for Western blot analysis. Some experiments were performed in the presence of inhibitors: Cells were incubated for 16 h with PTX (100 ng·ml^{-1}), 10 min with Y-27632 (10 μM) or 5 min with YM-254890 (10 μM) before stimulation by chymotrypsin. In some cases, cells were incubated with a combination of PTX and YM-254890.

For PAR1 disarming experiments, PAR2$^{-/-}$ CMT93 cells were first incubated with 1 U·ml^{-1} of chymotrypsin or its vehicle (HBSS) for 2 min at 37°C. After being washed once with HBSS, the cells underwent a second treatment with 10-U·ml^{-1} thrombin, 25-μM TFLLR or their vehicle (water) for 5 min at 37°C. Cell lysis and protein extract preparation were then performed as described above. Equal amounts of total proteins (5 μg, according to BCA protein assay) were separated by SDS–polyacrylamide gel electrophoresis (PAGE) on 4%–15% Mini-PROTEAN® TGX™ Precast Gels (Bio-Rad, Hercules, CA, USA) and transferred to nitrocellulose membranes. After blocking in PBS containing 0.2% Tween 20 and 5% milk, p42/p44 MAPK phosphorylation was detected using anti-phospho-p42/p44 rabbit monoclonal IgG (Cell Signaling Technology, Danvers, MA, USA, #4370) diluted 1/2000 in blocking buffer and incubated overnight at 4°C. Bound anti-phospho-p42/p44 was probed with horseradish peroxidase (HRP)-conjugated anti-rabbit antibodies (Promega, W401B) diluted at 1/3000 in blocking buffer. Peroxidase activity was visualized upon the addition of enhanced chemiluminescence (ECL) Western blotting reagents (GE Healthcare, Chicago, IL, USA) using a ChemiDoc MP Imaging System (Bio-Rad). The membranes were stripped for 20 min using a buffer containing 1% SDS, 0.1% Tween 20, 15-g·L^{-1} glycine and 0.37% HCl, washed with PBS–Tween 0.2% and incubated in blocking buffer for 1 h. The absence of residual signal was systematically verified by ECL. To normalize the phosphorylated p42/44 signals, the membranes were probed overnight at 4°C with a rabbit anti-p42/44 antibody recognizing both phosphorylated and unphosphorylated forms (Cell Signaling Technology, #9102) detected as described above. Image Lab Software 6.1 (Bio-Rad) was used to quantify the densitometric analyses of the p42/44 signals.

2.11 | Detection of chymotrypsin in human and mouse samples by Western blot

For the following Western blot experiments, different amounts of protein extracts from murine and human gut samples (see below) were loaded to adapt to different chymotrypsin abundance among the samples and to avoid signal saturation. The amount of loaded proteins prepared in Laemmli buffer was as follows: 2 and 0.1 μg for

human and murine pancreas, respectively; 25 and 17 μg for human and mouse faeces, respectively; and 40, 50 and 7 μg for murine colonic scrapings, human mucus and human colonic biopsy, respectively. Protein extracts were then resolved on 4%–15% gradient acrylamide gels as described in the previous section. Regarding migration, transfer, blocking, ECL detection, steps were carried out as described above. We systematically performed a first incubation with the secondary antibody alone in order to verify the absence of cross-reactivity of this antibody. After this validation, the membranes were incubated with the primary antibody followed by the secondary antibody. To avoid nonspecific binding, different antibodies were used for human and murine samples. For human samples, the primary antibody was an anti-chymotrypsin B 1/2 (CTRB1/2) mouse monoclonal IgG (D-5, Santa Cruz Biotechnology, sc-393414), and the secondary antibody was an HRP-coupled goat anti-mouse IgG (Jackson ImmunoResearch, West Grove, PA, USA, 115-035-166). For murine samples, we used an anti-CTRB1/2 goat monoclonal IgG (F-13, Santa Cruz Biotechnology, sc-161496) followed by an HRP-coupled donkey anti-goat IgG (Promega, V8051).

2.12 | Assay of chymotryptic proteolytic activity

Specific chymotrypsin activity was measured in murine stool and colonic scraping extracts by following the degradation of the chymotrypsin peptide substrate, Suc–Ala–Ala–Pro–Phe–AMC; 50 μl of extracts was placed in a 96-well plate and pre-incubated for 20 min at 37°C. The enzymatic reaction was started by adding an equal volume of 1-mM substrate solution (diluted in 100-mM Tris–HCl [pH 8] and 1-mM $CaCl_2$) to the samples. Substrate cleavage, leading to free AMC release, was monitored by measuring fluorescence (excitation: 360 nm; emission: 460 nm) every 30 s for 20 min in a Varioskan Flash microplate reader (Thermo Fisher Scientific). The initial velocities of the curves were extracted from the kinetic graphs using the SkanIt™ software (Thermo Fisher Scientific). The presence of a specific chymotrypsin-like activity in the samples was confirmed by comparison with the values obtained in the presence of the selective inhibitor chymostatin (500 μM). The proteolytic activity was quantified in $U \cdot ml^{-1}$ using a standard curve generated with increasing concentrations of commercial pancreatic chymotrypsin. Proteolytic activity was normalized to protein content measured with a BCA protein assay.

The same protocol was used to measure proteolytic activity in human stool and mucus extracts except that 1-mM CHAPS detergent was added to buffer for the dilution of the extracts, substrates and commercial chymotrypsin.

2.13 | Luciferase assay for measuring release of N-terminally tagged PARs

The ability of chymotrypsin to cleave and release the N-terminal domain of PAR1 and PAR2 was assessed essentially as described previously (Mihara et al., 2016), using CHO cells stably expressing hPAR1 or hPAR2 with a luciferase tag on the N-terminal extremity, and luciferase activity was monitored in the cell medium as follows: CHO–nLuc–PAR1 or PAR2 was plated in a 96-well plate at 20,000 cells per well and cultured for 48 h. The cells were then washed three times with HBSS and incubated with increasing concentrations of chymotrypsin for 10 min at 37°C. After exposure to chymotrypsin, cell supernatants potentially containing the cleaved PAR N-terminus (with nLuc tag) were collected, and proteolytic activity was stopped by adding 1 mM of the broad-spectrum serine inhibitor AEBSF. Any contaminating cell debris was removed by centrifugation for 5 min at 160 g. Using a Varioskan plate reader, luciferase activity was assayed in 50 μl of cell supernatant by recording luminescence for 5 min in white 96-well plates after the addition of 50 μl of the luciferase substrate provided in a luciferase assay kit (Nano-Glo® Luciferase Assay System, N1110, Promega). Luciferase signals were proportional to the amount of PAR cleaved on the cell surface. Luciferase release by chymotrypsin was normalized to the total bioluminescence yielded by untreated cells.

2.14 | Calcium mobilization assay

qCMT93 cells (WT or $PAR2^{-/-}$) were plated at 20,000 cells per well in black clear-bottom 96-well plates (Greiner Bio-One, 655090) and grown for 48 h. Cells were washed two times in HBSS (Gibco, 14025092) and incubated for 1 h at 37°C with 100 μl of Fluo-8 calcium probe (Screen Quest™ Fluo-8 Calcium AAT Bioquest®, Pleasanton, CA, USA) prepared following the manufacturer's recommendations. After one wash in HBSS, 100 μl of HBSS was added, and the cells were stimulated at 37°C while simultaneously monitoring calcium signals using an injector-equipped microplate reader (NOVOstar, BMG Labtech, Ortenberg, Germany). For all the experiments performed in the absence of extracellular calcium, Ca^{2+}-free HBSS (Gibco, 14175095) supplemented with 20-μM EGTA was used during cell stimulations. The recording of the calcium response started 4 s before cell stimulation (corresponding to the baseline values) and lasted up to 200 s. Curves were normalized by dividing each value by the baseline value, so each graph starts at 1. In some experiments, cells were stimulated twice.

For some experiments, inhibitors or antagonists were added before stimulation with chymotrypsin and were continually present until the end of the experiment. The PAR1 antagonist F16357 was added 5 min before cell stimulation by chymotrypsin. For G protein inhibition, cells were incubated for 16 h with PTX (100 $ng \cdot ml^{-1}$), 10 min with Y-27632 (10 μM) or 5 min with YM-254890 (10 μM). The intracellular calcium chelator BAPTA-AM was used at 30 μM and incubated for 1 h with cells prior to stimulation with chymotrypsin; its vehicle was 0.03% DMSO. To determine the involvement of the Ca^{2+} release-activated Ca^{2+} channel (CRAC) in the calcium response, cells were first incubated for 30 min with 10 μM of the CRAC antagonist, BTP2 (vehicle: 0.04% DMSO). Cells were then stimulated with chymotrypsin in calcium-free HBSS. Recording was done every 2 s, and an injection of $CaCl_2$ solution was done 4 min after the chymotrypsin

treatment in order to reach a 2-mM calcium concentration, enabling calcium influx from the medium to the cell cytoplasm. The magnitude of this calcium influx was quantified by calculating the area under the curve (AUC).

For HEK cells, measurements of calcium signalling induced by synthetic agonist peptides were conducted essentially as described previously (Kawabata et al., 1999; Mihara et al., 2016). Briefly, cells were lifted from a culture flask with EDTA-supplemented calcium-free isotonic PBS (pH 7.4), washed and resuspended at approximately 5.10^7 cells/ml in HBSS supplemented with 10-mM HEPES, 1.5-mM $CaCl_2$ and 1.5-mM $MgCl_2$ containing Fluo-4 calcium indicator (Thermo Fisher Scientific). Agonists were added to 2-ml stirred cell suspensions in a spectrofluorometer (PerkinElmer, Waltham, MA, USA), and the fluorescence emission signal at 530 nm (excitation wavelength: 480 nm) was measured to follow the intracellular calcium response.

2.15 | Statistical analyses

All graphical figures and statistical analyses were performed with the GraphPad Prism 9.4.1 software (GraphPad Software, San Diego, CA). For single comparisons, statistical differences were assessed with the nonparametric Wilcoxon matched-pairs signed-rank test. For multiple comparisons, the Friedman test was used, followed by Dunn's test for multiple comparisons. For disarming experiments, different concentrations of chymotrypsin were tested independently for technical reasons; thus, a Kruskal–Wallis test was employed followed by Dunn's post-test. In all cases, the significance level was fixed at $P < 0.05$. Regarding PAR1 and PAR2 cleavage experiments and PAR1 disarming, concentration–response curves were fitted in GraphPad with log transformation of the chymotrypsin concentrations followed by a non-linear regression for normalized responses with a standard Hill slope of 1 (agonist) or −1 (inhibition). The data and statistical analysis comply with the recommendations of the *British Journal of Pharmacology* on experimental design and analysis in pharmacology (Curtis et al., 2022).

2.16 | Nomenclature of targets and ligands

Key protein targets and ligands in this article are hyperlinked to corresponding entries in http://www.guidetopharmacology.org and are permanently archived in the Concise Guide to PHARMACOLOGY 2023/24 (Alexander, Christopoulos, et al., 2023; Alexander, Fabbro, et al., 2023; Alexander, Mathie, et al., 2023).

3 | RESULTS

3.1 | The epithelium is exposed to chymotrypsin activity throughout the intestinal tract

Chymotrypsin has been shown to adsorb easily to the surface of small IECs without loss of activity (Goldberg et al., 1968). However,

such proximity has never been addressed in the colon where the epithelium is covered by a thick mucus layer. In this context, we first explored the presence of chymotrypsin in protein extracts of different mouse and human colonic compartments by Western blot analyses. We used antibodies directed against the major pancreatic chymotrypsin form, chymotrypsin B (CTRB). As shown in Figures 1a and S2, in murine pancreatic extracts, we confirmed the presence of a unique signal at 26 kDa that corresponds to the molecular weight of CTRB. As expected, no such signal was detected in the lung because this organ does not express CTRB. In colonic compartments, we found that the CTRB band was immunodetected in stools as well as in colonic mucosal scrapings, but only when the mucosa-associated material, including the mucus layer, was preserved (unwashed). The CTRB signal was indeed not observed in mucosal scrapings obtained after extensive elimination of the luminal material. This result shows that the colonic mucosa is not an endogenous producer of CTRB and that this enzyme does not penetrate the epithelium. Similar results were found in human samples, where a specific CTRB signal was clearly visible not only in stools but also in colonic mucus, whereas the human colonic mucosa was negative for CTRB (Figures 1a and S2). Immunofluorescence experiments confirmed the detection of CTRB at the surface of the murine colonic epithelium, which was confined to the luminal content (Figure S3). These results highly suggest that in physiological conditions, chymotrypsin infiltrates the mucus layer and may reach the surface of the mouse and human colonic epithelium.

To assess whether the chymotrypsin protein detected in the different gut compartments was active, we measured chymotrypsin proteolytic activity by enzymatic assay (Figure 1b). Using Suc–Ala–Ala–Pro–Phe–AMC substrate, we found that human and mouse stools contained a substrate-cleaving activity that was fully inhibited by chymostatin, a specific inhibitor of chymotrypsin-like activities. As well, chymotrypsin activity was also detected in unwashed mucosal scrapings from mouse and human mucus. Altogether, our data highlight the presence of active chymotrypsin in the vicinity of the colonic epithelium in both mouse and human. In addition to the small intestine, these findings support that an interaction between chymotrypsin and the surface of IECs might also occur in the distal segments of the gastro-intestinal tract.

3.2 | Chymotrypsin cleaves PAR2 and activates calcium signalling in IECs

Due to the presence of active chymotrypsin neighbouring the small intestinal and colonic mucosa, we investigated the possible regulation of PARs by chymotrypsin. We focused on PAR1 and PAR2, which are both expressed at the apical surface of IECs (Bohm et al., 1996; Cenac et al., 2002; Cuffe et al., 2002; Kong et al., 1997; Lau et al., 2011).

We first assessed the ability of chymotrypsin to cleave the extracellular domain of PAR2. To do so, CHO cells stably expressing the PAR2 receptor fused to an nLuc tag on its N-terminal extremity were
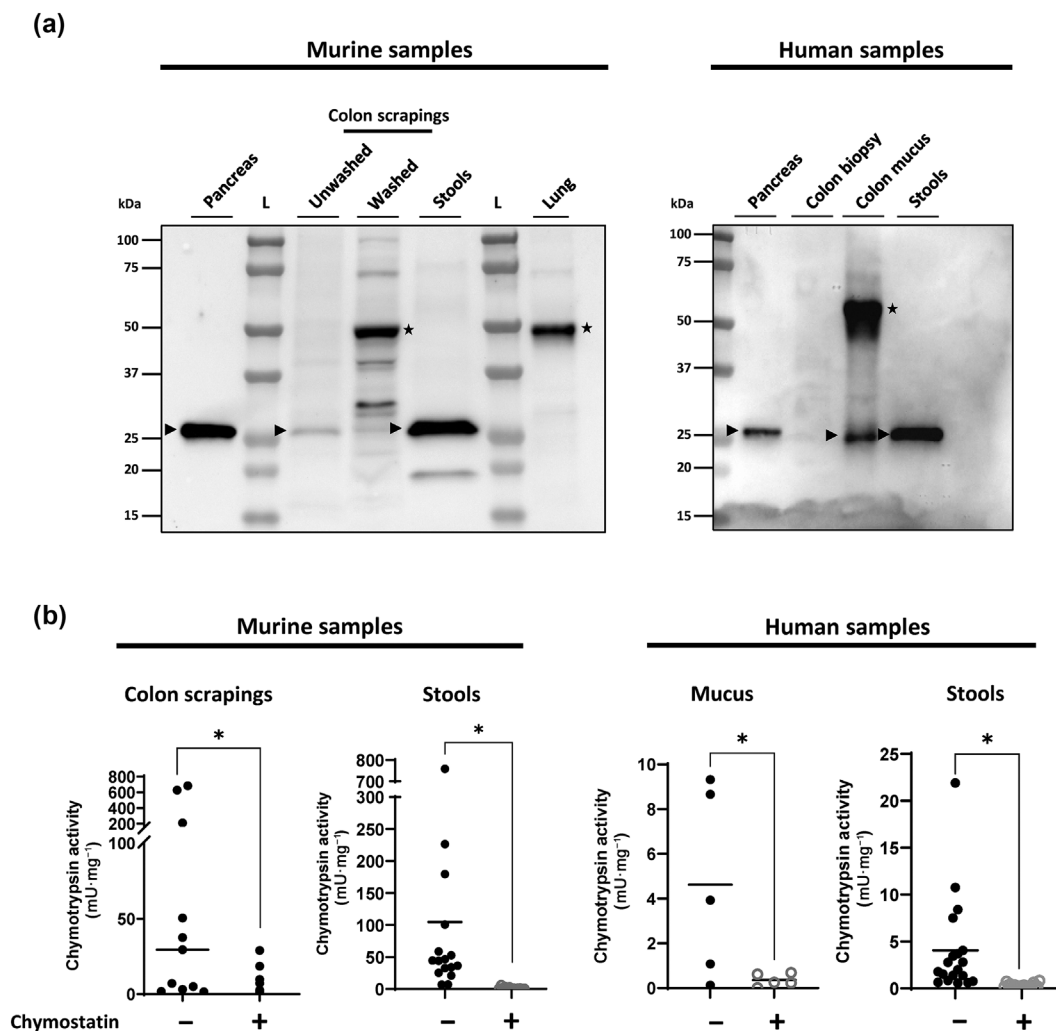
FIGURE 1 The colonic epithelium is exposed to chymotrypsin activity. (a) Immunodetection of chymotrypsin B (CTRB) in different gut sub-compartments from mouse samples (left panel) and human samples (right panel) by Western blot. Human and murine pancreas were used as positive controls for CTRB expression (26 kDa), and murine lung was used as a negative control. Different amounts of protein extracts were loaded to adapt to different chymotrypsin abundances among the samples and to avoid signal saturation: 2 and 0.1 μg for human and murine pancreas, respectively; 25 and 17 μg for human and mouse faeces, respectively; and 40, 50 and 7 μg for murine colonic scrapings, human mucus and human colonic biopsy, respectively. L: Ladder (Precision Plus Protein Dual Color standards [Bio-Rad]). Arrowheads point to CTRB signals. Of note, nonspecific signals (star) were visible in protein extracts from murine lung, scraping from washed mucosa and human mucus. The exploration of the origin of these nonspecific signals is reported in Figure S2. (b) Quantification of chymotrypsin-like activities in human and mouse gut sub-compartment samples. Mouse colonic scrapings and stools as well as human mucus and stools were extracted in native conditions, and the chymotrypsin-like activities were assayed using Suc–Ala–Ala–Pro–Phe–AMC as a substrate. The extracts were incubated with or without chymostatin (500 μM), a specific chymotrypsin-like inhibitor. The initial velocity of the curves was extracted from the kinetic graphs, and the graphs represent the chymotrypsin-like activity in mU·mg^{-1} protein for each sample. Each dot represents one patient or one mouse (n = 5 and 19 patients for human mucus and stool samples, respectively; n = 16 and 11 for mouse stool and scrap samples, respectively). *$P < 0.05$ (Wilcoxon matched-pairs signed-rank test).

treated with active chymotrypsin. As shown in Figure 2a, incubation of chymotrypsin with the reporter cells led to the release of luciferase activity into the culture medium in a concentration-dependent manner. These data show that chymotrypsin is able to cleave within the N-terminal extremity of PAR2.

We next investigated the ability of chymotrypsin to induce calcium mobilization downstream of PAR2 cleavage in IECs. We used the CMT93 colonic epithelial cell line that endogenously expresses high levels of PAR2 (Nasri et al., 2016). As illustrated in Figure 2b,

chymotrypsin was able to generate concentration-dependent calcium signalling in WT CMT93 cells. This calcium response was completely abolished when PAR2-deficient (PAR2$^{-/-}$) cells were used. In addition, the use of a PAR2 antagonist (I-191 at 10 μM) drastically reduced the calcium response (Figure 2c). These experiments reveal that chymotrypsin drives calcium signalling in intestinal epithelial CMT93 cells exclusively via PAR2.

We then employed inhibitors against the different Gα protein subunits known to be recruited downstream of PAR2 activation
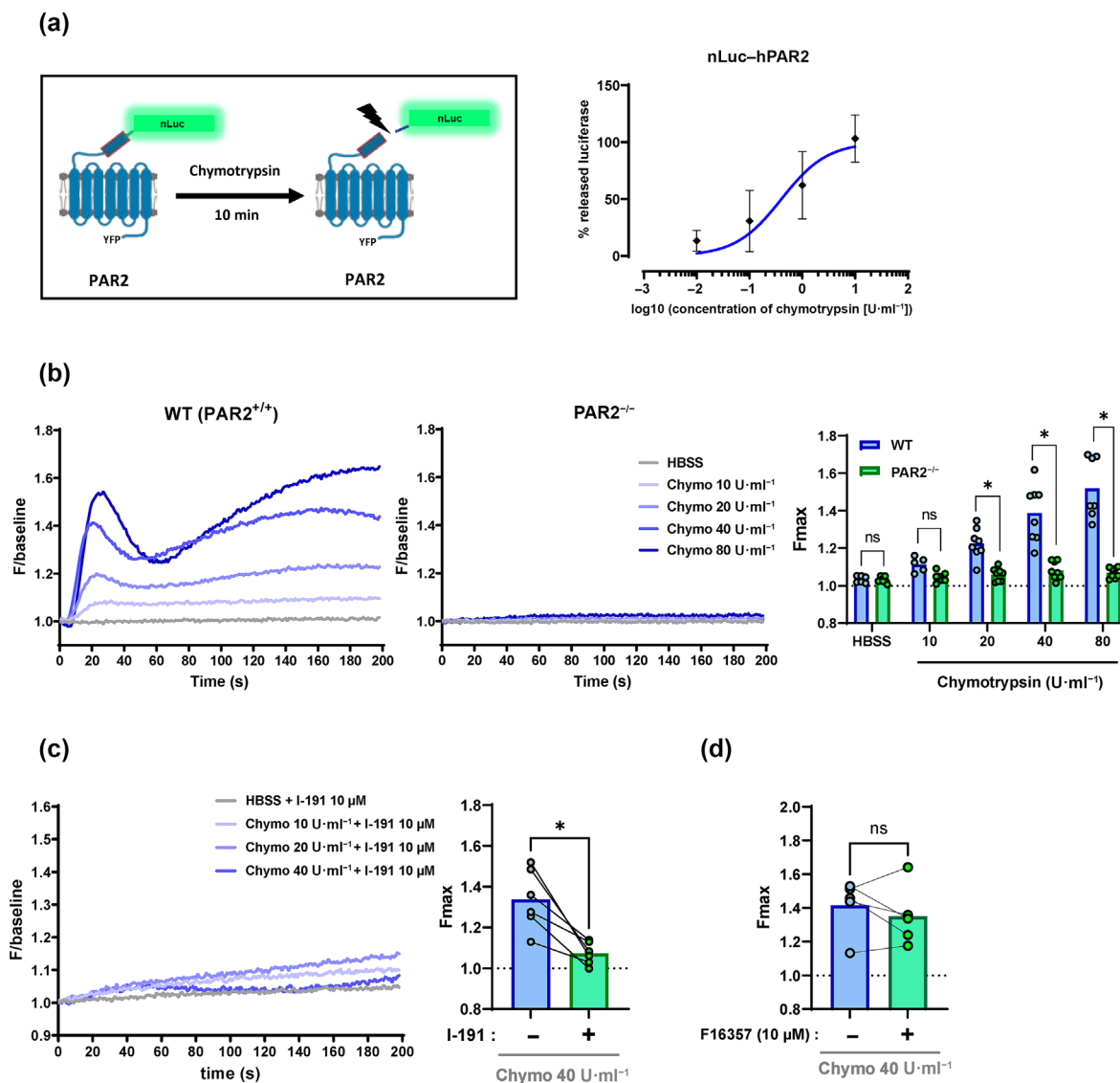
FIGURE 2 Chymotrypsin cleaves PAR2 and induces calcium signalling in CMT93 intestinal epithelial cells. (a) Cleavage quantification of the extracellular domain of PAR2. CHO cells stably expressing nanoluciferase–hPAR2–YFP were incubated with increasing amounts of chymotrypsin for 10 min. Luciferase activity was measured in the supernatant and divided by the total luciferase activity present in untreated cells. The graph represents the mean ± SD of the % of released nanoluciferase activity as a function of chymotrypsin concentration (transformed in $\log_{10}$). A curve with a standard slope (Hill slope = 1) is represented. The graph represents five independent experiments. (b) Calcium mobilization assays using Fluo-8-loaded CMT93 cells treated with increasing amount of chymotrypsin. Injection of chymotrypsin (Chymo) or vehicle (HBSS) was performed at 4 s. The fluorescence of the calcium Fluo-8 probe was recorded over 200 s and represents the fluorescent level normalized by the baseline level (F/baseline), which is the level of fluorescence before injection. The calcium response observed in WT CMT93, expressing PAR2 endogenously, was totally abolished in PAR2$^{-/-}$ cells. The maximum fluorescence values (F_{max}) obtained for each concentration of chymotrypsin (right panel) were compared between PAR2$^{+/+}$ and PAR2$^{-/-}$ cells. Each dot on the plot represents one independent experiment (HBSS: n = 8; WT: 10 U·ml^{-1}, n = 5; PAR2$^{-/-}$: 10 U·ml^{-1}, n = 7; 20 U·ml^{-1}, n = 8; and 40 U·ml^{-1}, n = 8; WT: 80 U·ml^{-1}, n = 7; PAR2$^{-/-}$: 80 U·ml^{-1}, n = 8) *P < 0.05 (Wilcoxon matched-pairs signed-rank test). (c) Calcium mobilization assays using Fluo-8-loaded CMT93 cells treated with an increasing amount of chymotrypsin and the PAR2 antagonist I-191 at 10 μM. The maximum fluorescence values (F_{max}) obtained with 40-U·ml^{-1} chymotrypsin in the presence or not of I-191 were quantified and compared (right panel, n = 6 independent experiments). (d) Calcium mobilization assays using Fluo-8-loaded CMT93 cells treated with 40-U·ml^{-1} chymotrypsin in the absence or presence of the PAR1 antagonist F16357 at 10 μM. The maximum fluorescence values (F_{max}) were quantified and compared (n = 5 independent experiments). Each dot on the plot represents one independent experiment; paired data are connected by a line. *P < 0.05; ns, non-significant (Wilcoxon matched-pairs signed-rank test).

(YM-254890 for G$_q$, PTX for G$_{i/o}$ or Y-27632 for Rho-dependent G$_{12/13}$). Pre-treatment of cells by PTX or Y-27632 had no effect on the chymotrypsin-induced calcium response, whereas YM-254890 prevented it (Figure 3). This indicates that the calcium mobilization triggered by chymotrypsin via PAR2 is totally dependent on G$_q$ proteins. Together, our results show that chymotrypsin activity is able to cleave PAR2 and trigger G$_q$-dependent calcium signalling in IECs.

FIGURE 3 G_q proteins, but not $G_{12/13}$ or $G_{i/o}$ proteins, are involved in the calcium signal downstream of PAR2 activation by chymotrypsin in CMT93 cells. Calcium mobilization assay using Fluo-8-loaded CMT93 cells treated with 40-$U \cdot ml^{-1}$ chymotrypsin (Chymo) or its dilution buffer (HBSS) after pre-incubation with G protein inhibitors: (a) YM-254890 (G_q inhibitor) at 10 μM for 5 min, (b) Y-27632 (Rho-dependent $G_{12/13}$ inhibitor) at 10 μM for 10 min or (c) pertussis toxin (PTX) (G_i inhibitor) at 100 $ng \cdot ml^{-1}$ for 16 h. Vehicles were 0.1% DMSO (a) or water (b, c). Profiles are representative of one experiment that was repeated five independent times minimum. The F_{max} obtained for each experiment was plotted on graphs (right-hand panels). *$P < 0.05$; ns, non-significant (Wilcoxon matched-pairs signed-rank test).
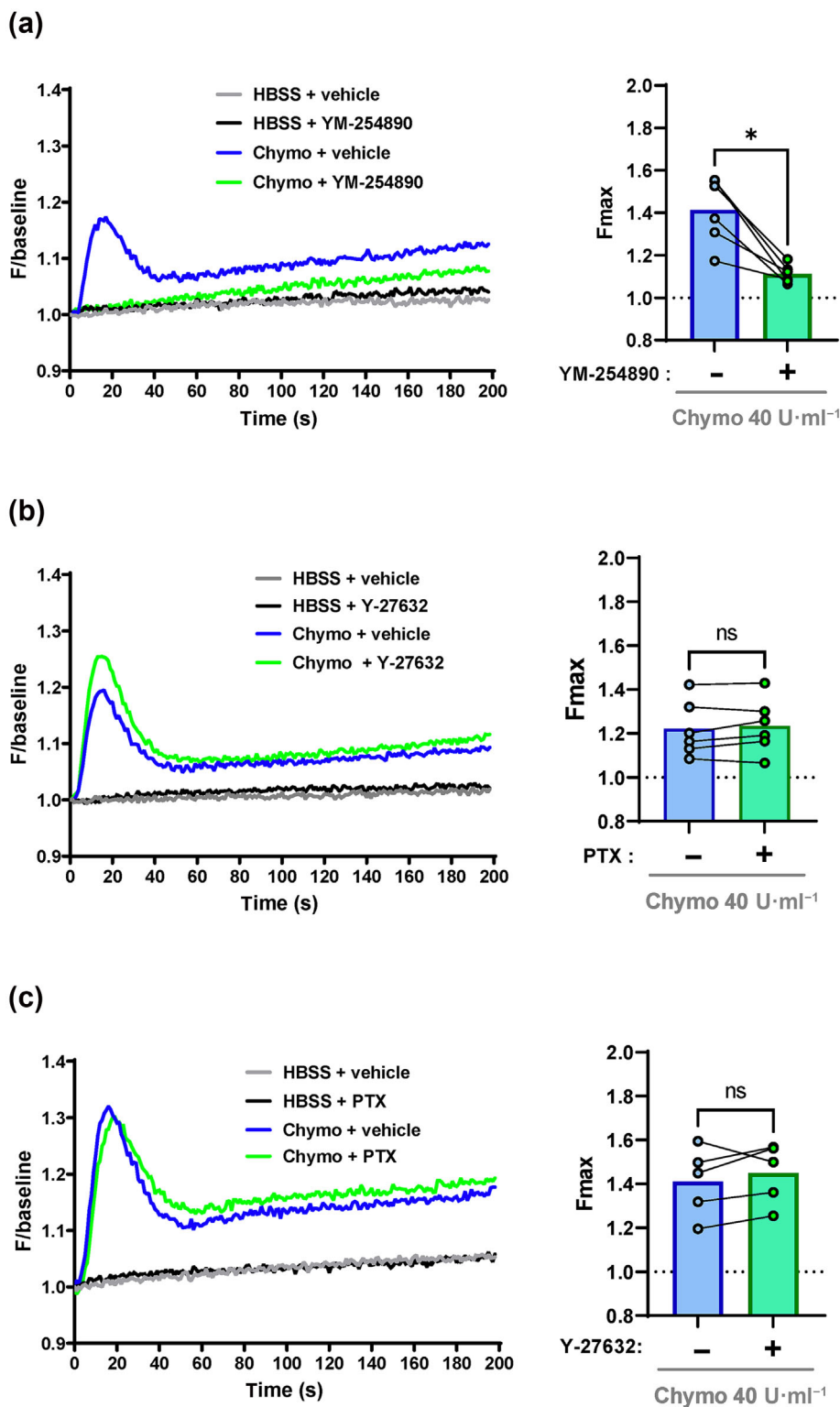
3.3 | PAR2 activation by chymotrypsin mediates store-operated calcium entry (SOCE) in CMT93 cells

Interestingly, the kinetics of the increase in intracellular calcium caused by chymotrypsin differed from the kinetics observed with the PAR2 canonical agonists trypsin or SLIGRL (cf. Figures 2b and S1B,C). These classical activators caused an early peak of intracellular calcium immediately followed by a decrease, without any increase afterwards. In contrast, with chymotrypsin, the first calcium peak was consistently followed by a sustained plateau or increasing phase of the calcium signal.

Then, we analysed in detail the chymotrypsin-induced calcium signal with the goal of determining the involvement of intracellular and/or extracellular calcium. The use of BAPTA-AM, a membrane-
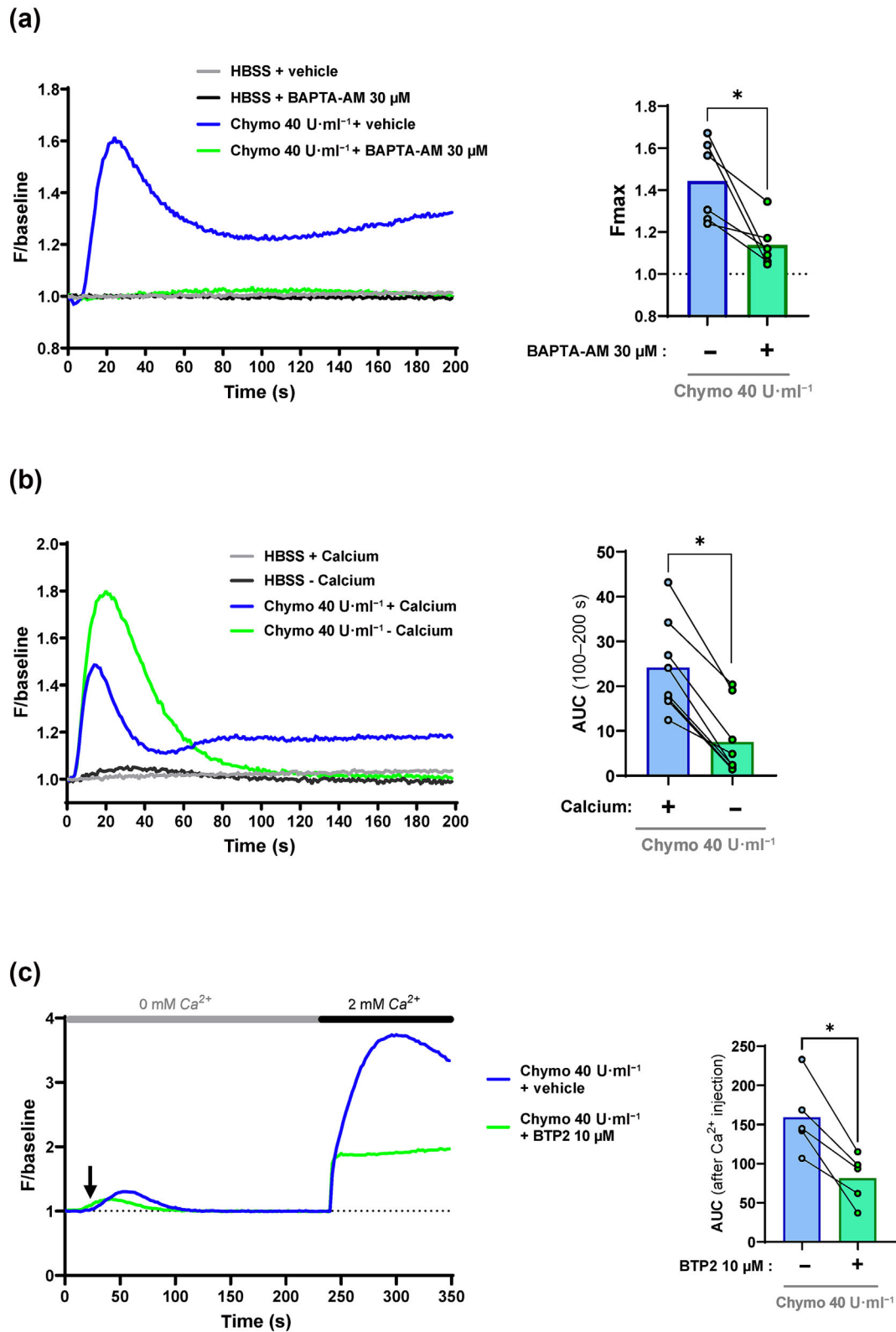
FIGURE 4 Legend on next page.

permeant chelator that traps intracellular calcium, prevented the signalling induced by chymotrypsin (Figure 4a), demonstrating that the chymotrypsin-induced calcium signal is dependent on release from calcium intracellular stores. Then, the use of a calcium-free medium during cell stimulation by chymotrypsin significantly lowered the plateau phase while maintaining the first peak of intracellular calcium (Figure 4b). These results strongly suggest that chymotrypsin induces a calcium response initiated by a release of calcium from intracellular stores followed by an influx of calcium from the extracellular medium.

We investigated the role of CRACs in this pathway. Indeed, these proteins belong to a family of plasma membrane calcium channels named Orai that are activated by intracellular store depletion via STIM sensors located in the endoplasmic reticulum (ER) membranes. The interaction between STIM and Orai proteins triggers channel opening and subsequent entry of extracellular calcium into the cytosol, a process called SOCE (Zhang et al., 2020). We found that all CRAC components—Orai1, Orai2 and Orai3 channels, as well as Stim1 and Stim2—were expressed in CMT93 cells (Figure S4). Therefore, we investigated the role of CRACs in the delayed calcium response using a two-step strategy to uncouple the intracellular store mobilization from the extracellular influx of calcium. As shown in Figure 4c, CMT93 cells were first stimulated with chymotrypsin (arrow) in the absence of extracellular calcium. As expected in these conditions, the protease triggered calcium mobilization from intracellular stores in cells (as previously observed in Figure 4b, calcium-free conditions). After returning to a basal fluorescence signal, the addition of a Ca^{2+} solution (2 mM final) in the extracellular medium resulted in a substantial entry of calcium into the cells. This calcium influx was quantified by calculating the AUC. Pre-treatment of cells with the CRAC antagonist BTP2 significantly reduced the amplitude of calcium influx, showing that chymotrypsin triggered CRAC activation downstream of PAR2 in CMT93 cells.

Altogether, our results showed the ability of chymotrypsin to cleave PAR2 and activate a G_q-dependent increase in intracellular calcium, which is composed of two phases: a first release from ER stores, followed by a CRAC-mediated SOCE from the extracellular environment.

3.4 | Chymotrypsin activates ERK1/2 signalling downstream of PAR2 in IECs

In addition to calcium signalling, we also evaluated whether chymotrypsin could activate the ERK1/2 pathway via PAR2 in CMT93 cells. For this purpose, we stimulated WT or PAR2$^{-/-}$ CMT93 cells for 10 min with different concentrations of chymotrypsin. The ratios between phosphorylated and total ERK1/2 were quantified by Western blot in the protein extracts to evaluate the ERK1/2 activation levels. Figure 5a shows the ability of chymotrypsin to activate the ERK1/2 signalling pathway specifically via PAR2 in CMT93 cells, because the absence of this receptor (PAR2$^{-/-}$) significantly reduced the ERK1/2 phosphorylation levels. As a control, heat-inactivated chymotrypsin was not able to trigger ERK1/2 activation. Finally, pretreatment of cells with PTX or YM-254890, but not with Y-27632, significantly reduced the PAR2-dependent ERK1/2 activation caused by chymotrypsin (Figure 5b). We observed a synergistic effect of the combined use of PTX and YM-254890 that fully abolished ERK1/2 signalling, as shown in Figure S5. Interestingly, in contrast to chymotrypsin, trypsin was still able to activate the ERK1/2 pathway in the absence of PAR2 (Figure S6). Our data also showed that trypsin could trigger an elevation of intracellular calcium in PAR2$^{-/-}$ CMT93 cells (Figure S1C). These results highlight functional differences between trypsin and chymotrypsin in terms of molecular targets at the cell surface.

Altogether, our data indicate that the cleavage of PAR2 by chymotrypsin induces an ERK1/2 signalling pathway involving the independent contribution of $G_{i/o}$ and G_q. In addition, in contrast to what was observed with trypsin, chymotrypsin-associated calcium and ERK1/2 signalling pathways are exclusively dependent on PAR2.

3.5 | Chymotrypsin cleaves PAR2-derived synthetic peptides at a non-canonical site in vitro but might use the canonical site in a cellular context

To determine the cleavage sites of PAR2 by chymotrypsin, we performed in vitro digestion of a synthetic hPAR2 N-terminal peptide (GTNRSSKGR**SLIGKV**DGTSHVTGKGVT-NH$_2$) encompassing the canonical TL sequence (**SLIGKV**) and determined the sequence of

FIGURE 4 CRACs are involved in the long-term calcium influx observed downstream of PAR2 activation by chymotrypsin (Chymo) in CMT93 cells. (a) Calcium mobilization assays of Fluo-8-loaded CMT93 cells stimulated with 40-U·ml^{-1} chymotrypsin or its dilution buffer (HBSS). A pretreatment of 1 h was carried out with the intracellular calcium chelator BAPTA-AM at 30 μM or its vehicle (0.03% DMSO). The experiment was performed six independent times, and the F_{max} of each experiment was reported on the right-hand graph. *$P < 0.05$ (Wilcoxon matched-pairs signed-rank test). (b) Calcium mobilization assays of Fluo-8-loaded CMT93 cells stimulated with 40-U·ml^{-1} chymotrypsin or HBSS, in the presence or absence of extracellular calcium (− calcium). The calcium influx occurring after the initial RE store mobilization was quantified using the area under the curve (AUC) from 100 to 200 s. The graph represents the AUC calculated from seven independent experiments. *$P < 0.05$ (Wilcoxon matched-pairs signed-rank test). (c) Calcium mobilization assays of Fluo-8-loaded CMT93 cells using a two-step strategy to uncouple the intracellular store mobilization from the extracellular influx. CMT93 cells were first stimulated with chymotrypsin (represented by an arrow) in calcium-free conditions (0-mM Ca^{2+}). The experiment was done in the presence or absence of the CRAC antagonist BTP2 at 10 μM or its vehicle (0.04% DMSO). Then, 240 s after the first stimulation, a CaCl$_2$ solution was added (2-mM Ca^{2+} final concentration). The curves show the results of one representative experiment repeated five independent times. Calcium influx was quantified by measuring the AUC following CaCl$_2$ injection (240–350 s). *$P < 0.05$ (Wilcoxon matched-pairs signed-rank test).
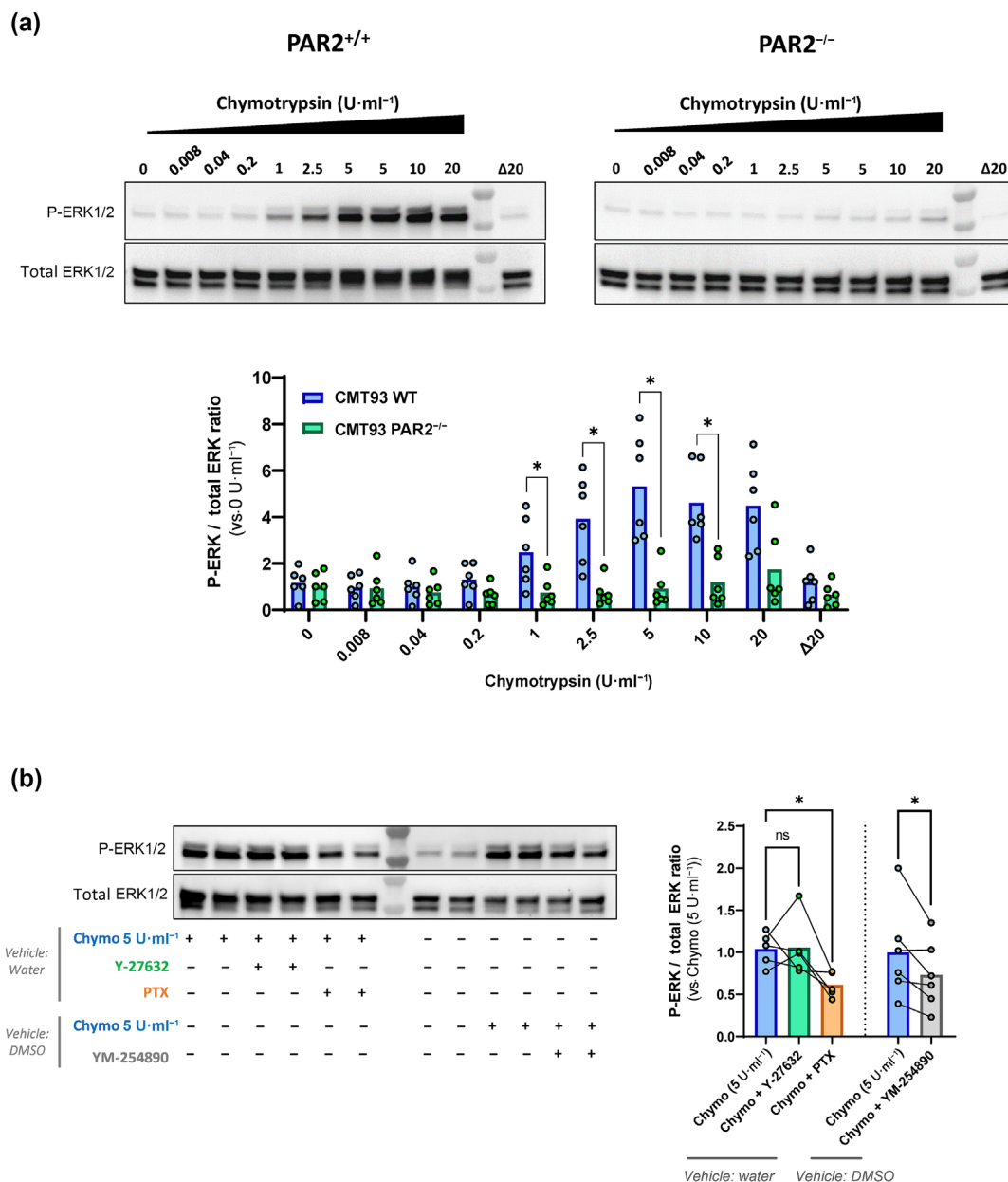
(a)

(b)

FIGURE 5 Chymotrypsin activates the ERK1/2 signalling pathway via PAR2, depending on G_q and $G_{i/o}$ proteins in intestinal epithelial cells. (a) Representative immunoblots of ERK1/2 phosphorylation in WT (PAR2$^{+/+}$) or PAR2$^{-/-}$ CMT93 cells. Cells were treated for 10 min with increasing concentrations of chymotrypsin (Chymo) (0–20 U·ml^{-1}). HBSS corresponded to 0 U·ml^{-1}. Heat-inactivated chymotrypsin (20 U·ml^{-1}) was used as a control (Δ20). Cell lysates were analysed by Western blot using anti-phosphorylated ERK1/2 (P-ERK) antibodies and then anti-total ERK1/2 antibodies. The ratios between P-ERK and total ERK signals were quantified by densitometric analysis and represented on the graph below the blots. Each dot on the plot represents one independent experiment (n = 6 independent experiments). *$P < 0.05$ (Wilcoxon matched-pairs signed-rank test). (b) ERK1/2 phosphorylation analysed by Western blot in WT CMT93 cells stimulated for 10 min with 5-U·ml^{-1} chymotrypsin after pre-incubation with G protein inhibitors: YM-254890 at 10 μM for 5 min, Y-27632 at 10 μM for 10 min or pertussis toxin (PTX) at 100 ng·ml^{-1} for 16 h. Pre-incubations with the corresponding vehicle solutions (0.1% DMSO for YM-254890 or water for Y-27632 and PTX) served as controls. The ratios between P-ERK and total ERK signals were quantified by densitometric analysis and represented on the right-hand panels. Each dot on the plot represents one independent experiment (n = 5 for experiments performed with PTX and Y-27632, n = 6 for YM-254890). *$P < 0.05$ (Wilcoxon test for single comparison [effect of YM-254890]; Friedman followed by Dunn's test for multiple comparisons [effects of Y-27632 or PTX]).

the generated cleavage products by high-performance liquid chromatography–mass spectrometry (HPLC–MS) analysis (Figure 6a). This peptide was incubated with 5-U·ml^{-1} chymotrypsin for 30 min.

The HPLC peak generated by chymotrypsin corresponded to a cleavage of the parental peptide two amino acids downstream of the trypsin canonical R^{36}/S^{37} cleavage site, that is, at L^{38}/I^{39}. This generated

FIGURE 6 Chymotrypsin cleaves PAR2 at the L^{38}/I^{39} site in vitro, but the canonical R^{36}/S^{37} site may drive calcium signalling *in cellulo*. (a) Determination of the cleavage sites of hPAR2 by chymotrypsin. The human PAR2 N-terminus-derived peptide was incubated with 5-U·ml^{-1} chymotrypsin at 37°C for 30 min, and the samples were fractionated by HPLC followed by MALDI/MS. The HPLC tracing indicates the presence of a cleavage site after L^{38} and generating the IGKVDGTSHVTGKGVT-NH$_2$ peptide (arrowhead). The sequence of the tethered ligand is underlined. (b) Calcium mobilization assay of Fluo-4-loaded WT HEK cells (expressing PAR1 and PAR2) or PAR2$^{-/-}$ HEK cells stimulated with 5-U·ml^{-1} chymotrypsin. (c) Calcium mobilization assay performed on double-deficient PAR1$^{-/-}$ and PAR2$^{-/-}$ HEK cells stably transfected with a vector encoding mutant hPAR2 (carrying a mutation at a canonical site [R^{36}G]). Cells were stimulated with 5-U·ml^{-1} chymotrypsin (left panel) or trypsin (right panel) and then by PAR2 agonist peptide 2-furoyl-LIGRLO-NH$_2$ (2fLI) (1 μM) as a positive control. The data in each panel are representative of five or more independent experiments.
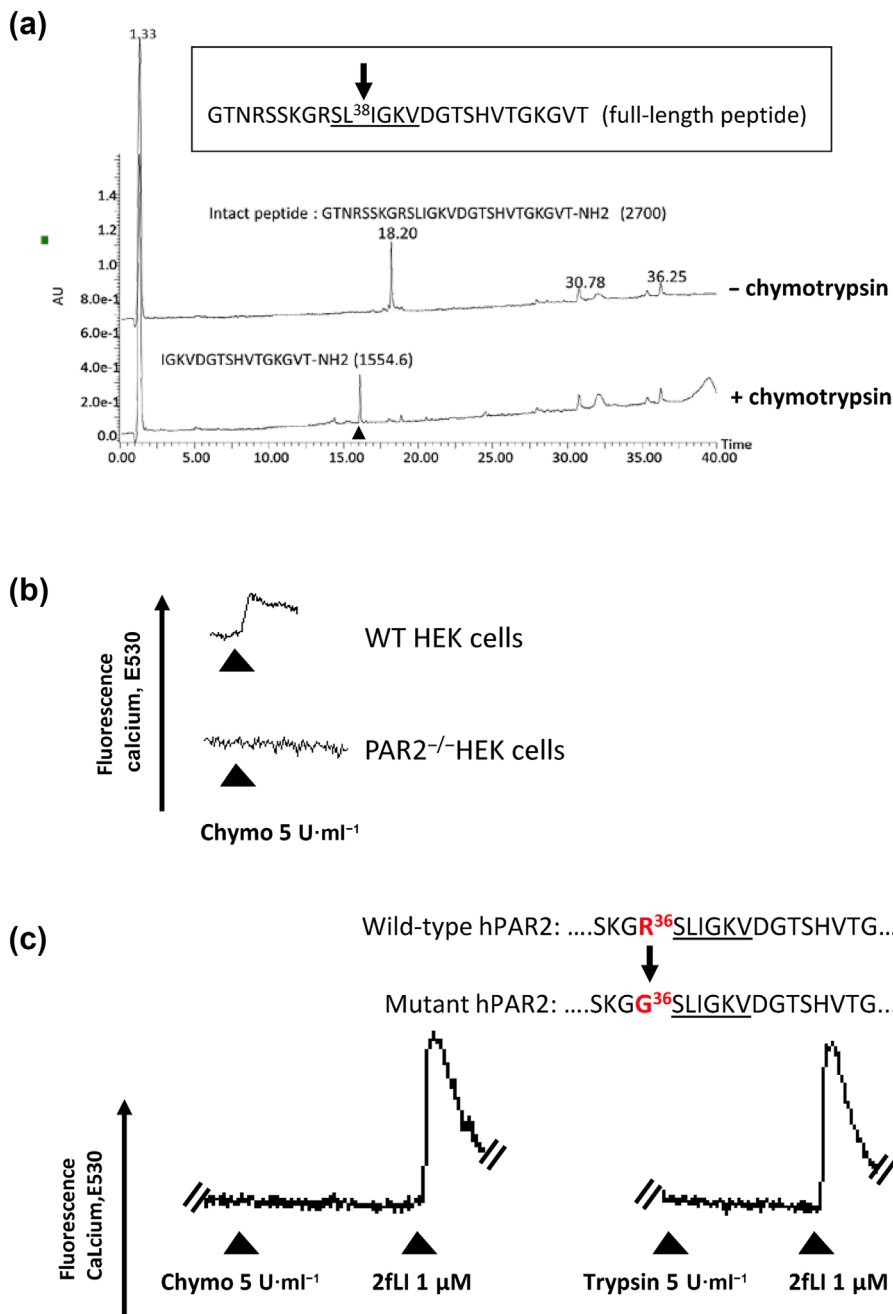
the **IGKV**DGTSHVTGKGVT-NH$_2$ C-terminal peptide, which lacks S^{37}–L^{38}. Intriguingly, the complementary N-terminal peptide (GTNRSSKGR**SL**) was not detected. We suspect that this peptide was rapidly digested by chymotrypsin during these experiments. The two amino acids S^{37}–L^{38} were described as essential to generate a PAR2-dependent calcium signalling in HEK cells (Ramachandran et al., 2009). We therefore reasoned that the L^{38}/I^{39} cleavage site, which removes S^{37}–L^{38}, was unlikely to generate the chymotrypsin-induced calcium response. We investigated this hypothesis using HEK cells, a human cell line widely used for the study of PAR pharmacology. We first validated that chymotrypsin was able to generate a calcium signal in WT HEK cells, with a plateau phase as observed in CMT93, which was totally abolished in PAR2$^{-/-}$ cells (Figure 6b). We

then constructed a mutant version of hPAR2 obtained after site-directed mutagenesis of WT hPAR2 sequence at the canonical site (R^{36}G). This construction was transfected in double-deficient PAR1 and PAR2 HEK cells. In those transfected cells, no calcium signal was observed upon stimulation by chymotrypsin or trypsin, while treatment with the PAR2 agonist peptide 2-furoyl-LIGRLO-NH$_2$ (2fLI) was still able to trigger a calcium response, validating the functionality of the transfected PAR2 R^{36}G mutant receptors (Figure 6c). These data highly suggest that, in contrast to what happens in the in vitro cleavage assay, chymotrypsin is cleaving at the canonical site of PAR2 to induce calcium signalling *in cellulo*. In line with this idea, our data revealed that neither a short (IGKVDGT-NH$_2$) nor a long (IGKVDGTSHVTGKGVT-NH$_2$) synthetic peptide, corresponding to

the sequence unmasked by the L^{38}/I^{39} cleavage site, activated calcium or ERK1/2 signalling in HEK cells (Figure S7).

Overall, our data suggest that chymotryptic activity is able to cleave PAR2 at the R^{36}/S^{37} and L^{38}/I^{39} sites, but only the R^{36}/S^{37} cleavage site appears to be responsible for the downstream activation of calcium and ERK1/2 signals in living cells.

3.6 | Chymotrypsin disarms PAR1

Because PAR1 is also expressed in IECs, we next explored the possible action of chymotrypsin on this receptor. As done for PAR2, the cleavage of the N-terminal domain of PAR1 was investigated by incubating CHO cells stably expressing nLuc–hPAR1 with increasing concentrations of chymotrypsin. As illustrated in Figure 7a, chymotrypsin was able to release N-terminal peptides containing luciferase from the tagged PAR1 in a concentration-dependent manner. The PAR1 cleavage site was then determined by in vitro digestion of a synthetic hPAR1 N-terminal peptide followed by HPLC–MS analysis. This experiment revealed a unique cleavage site localized within the canonical TL sequence, at F^{43}/L^{44} (Figure 7b). To investigate the consequences of PAR1 cleavage by chymotrypsin, we took advantage of PAR1 expression and functionality in WT and PAR2$^{-/-}$ CMT93 cells (Nasri et al., 2016). As inferred from our experiments in PAR2-deficient (but PAR1-expressing) CMT93 cells, the cleavage of PAR1 by chymotrypsin did not generate any signalling (Figures 2b and 5a). According to these results, we hypothesized that the chymotrypsin-mediated cleavage of PAR1 within the TL sequence would disarm rather than activate the receptor.

We therefore investigated the possibility for chymotrypsin to impede further cleavage and signalling induced by thrombin, the canonical activator of PAR1, known to cleave at the R^{41}/S^{42} site to unmask the TL SFLLR. In PAR2$^{-/-}$ CMT93, we showed that the thrombin-induced calcium response is totally attributable to PAR1 because the use of the PAR1 antagonist F16357 totally abolished the calcium response (Figure 8a). In order to test the ability of chymotrypsin to prevent the PAR1-mediated calcium response induced by thrombin, we carried out sequential incubations with chymotrypsin and then thrombin (Figure 8b). To prevent the possible degradation of thrombin by chymotrypsin, chymotrypsin was removed before the addition of thrombin. Figure 8c illustrates the calcium response recorded during the second stimulation of CMT93 cells with thrombin (or HBSS). As a positive control, the pre-incubation of cells with thrombin fully prevented the calcium response induced by a second stimulation with thrombin, due to the desensitization of the receptor (Figure 8c,d). Similarly, the pre-incubation of cells with 10-U·ml^{-1} chymotrypsin totally abolished the calcium response normally induced by thrombin. This disarming effect was concentration-dependent as illustrated in Figure 8e,f, with an IC$_{50}$ of 0.02 U·ml^{-1}. The functionality of PAR1 in cells pre-treated or not with chymotrypsin remained intact because calcium responses upon addition of TFLLR, the PAR1 agonist peptide, were not significantly impacted (Figure 8g).

Thrombin is also known to activate the ERK1/2 pathway downstream of PAR1 cleavage (Mihara et al., 2013; Wang et al., 2002), which we confirmed using our PAR2$^{-/-}$ CMT93 cell model by Western blot (Figure 8h). Interestingly, as observed for calcium signalling, the disarming effect of chymotrypsin towards PAR1 was also clearly observable for ERK1/2 signalling.

Taken together, our study shows that chymotrypsin does not activate PAR1, but instead prevents thrombin-dependent signalling pathways by cleaving PAR1 two amino acids downstream of the canonical cleavage site.
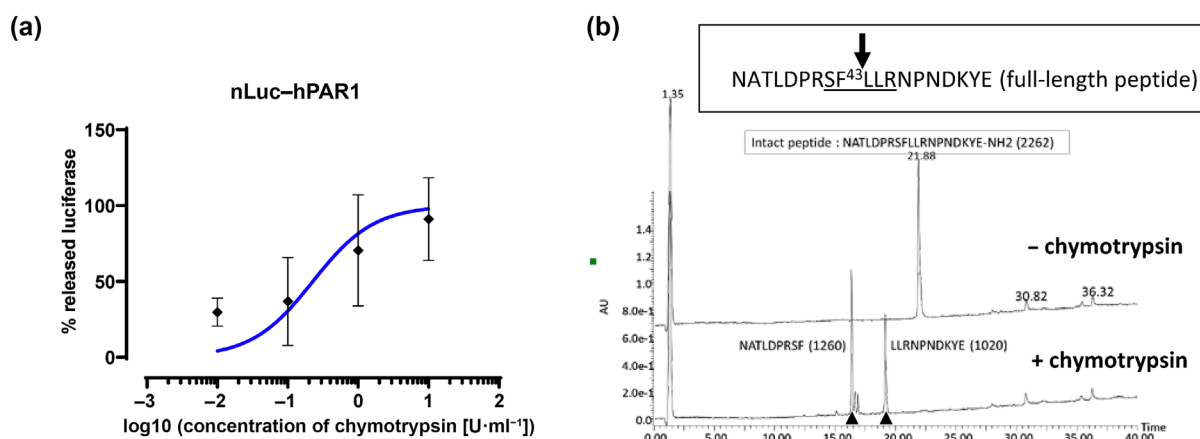
(a)

nLuc–hPAR1

(b)

NATLDPRS$\underline{F^{43}}$\underline{LLR}NPNDKYE (full-length peptide)

FIGURE 7 Chymotrypsin cleaves the N-terminal extremity of PAR1. (a) Cleavage quantification of the N-terminal domain of PAR1. CHO cells stably transfected with nLuc–hPAR1–YFP were incubated for 10 min with increasing amounts of chymotrypsin (0–10 U·ml^{-1}). Luciferase activity was measured in the supernatant and divided by the total luciferase activity of the cells. The graph represents the mean ± SD of the % of released nanoluciferase activity as a function of chymotrypsin concentration (transformed in log$_{10}$). A curve with a standard slope (Hill slope = 1) was represented. The graph represents five independent experiments. (b) Determination of the cleavage sites of hPAR1 by chymotrypsin. The human PAR1 N-terminus-derived peptide was incubated in the absence (− chymotrypsin) or presence of 5-U·ml^{-1} chymotrypsin (+ chymotrypsin) for 30 min at 37°C, and the samples were fractionated by HPLC followed by MALDI/MS. HPLC–MS analysis indicates the presence of two peptides derived from the full-length parental peptide (arrowheads) and reveals a unique and unambiguous cleavage site after F^{43}, two amino acids after the canonical cleavage site. The sequence of the tethered ligand is underlined. The profile is representative of five or more experiments.
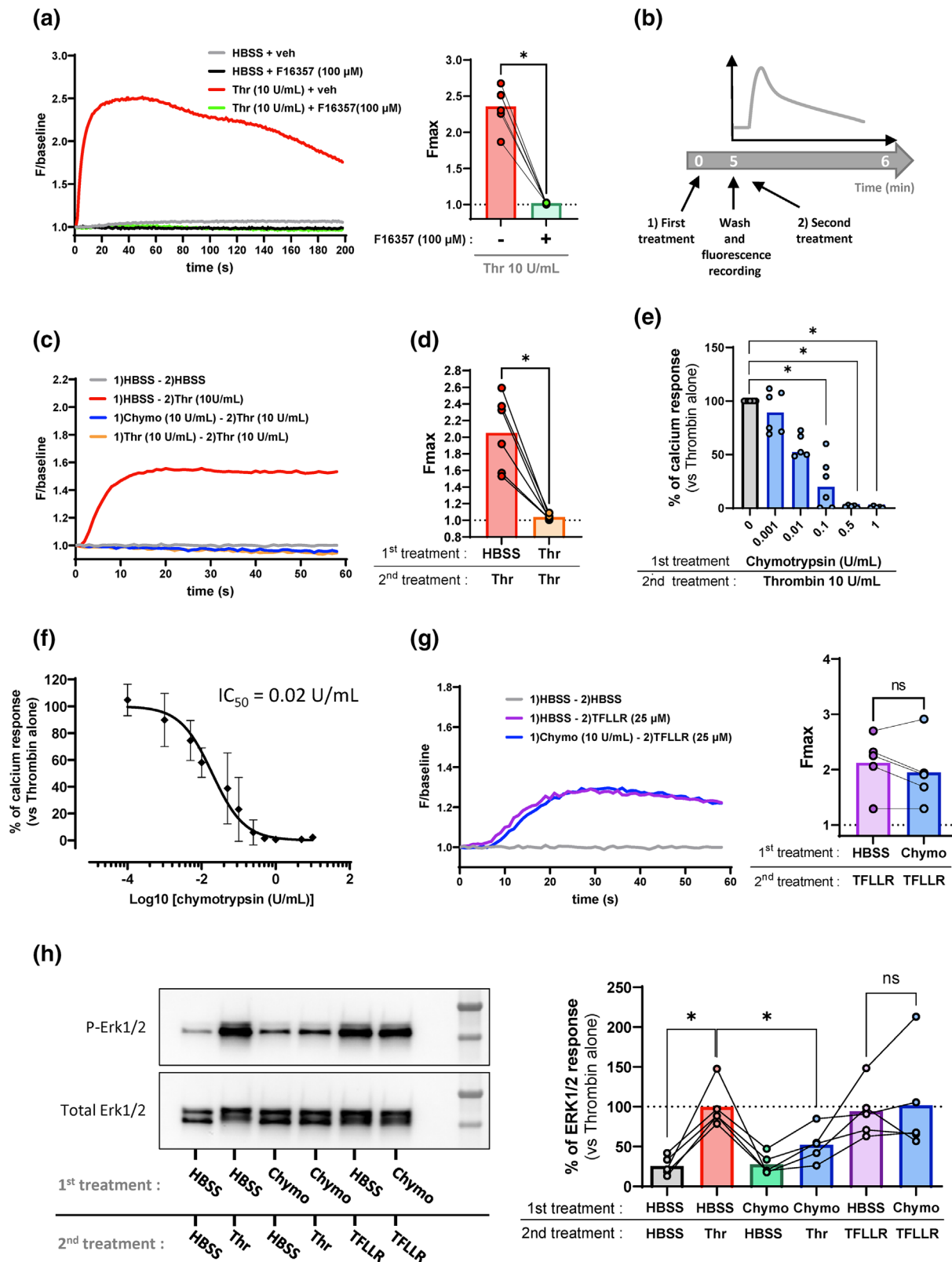
FIGURE 8 Legend on next page.

FIGURE 8 Chymotrypsin (Chymo) disarms PAR1 in intestinal epithelial cells. (a) Calcium flow experiments performed in Fluo-8-loaded PAR2$^{-/-}$ CMT93 cells (expressing PAR1 endogenously). Cells were stimulated with 10-U·ml^{-1} thrombin (Thr) or its dilution buffer (HBSS) with or without the PAR1 antagonist F16357 at 100 μM. Vehicle (veh): 0.5% DMSO. The maximum fluorescence value (F_{max}) obtained with thrombin ± F16357 for each experiment is reported on the right-hand graph (n = 6 independent experiments). *$P < 0.05$ (Wilcoxon matched-pairs signed-rank test). (b) Experimental design of PAR1 disarming experiments. Fluo-8-loaded PAR2$^{-/-}$ CMT93 cells were first treated with chymotrypsin or HBSS (1). Five minutes later, the cell supernatant was replaced by HBSS, and the recording of the calcium signal started. A second stimulation (2) was performed with 10-U·ml^{-1} thrombin or 25-μM PAR1-activating peptide (TFLLR), and the calcium signal was recorded for 60 s. (c) Representative calcium response curves of PAR1 disarming by chymotrypsin (blue line) and desensitization by thrombin in PAR2$^{-/-}$ CMT93 (orange line). Double treatment with HBSS was used as a control (grey line). (d) Quantification of thrombin-induced PAR1 desensitization. The F_{max} values were quantified and reported on the graph (n = 6 independent experiments). *$P < 0.05$ (Wilcoxon matched-pairs signed-rank test). (e) Quantification of the chymotrypsin-induced PAR1 disarming effect. PAR2$^{-/-}$ CMT93 cells were pre-incubated with an increasing amount of chymotrypsin and then stimulated with thrombin during calcium mobilization assays as explained in (b). The F_{max} induced by thrombin after incubation with chymotrypsin was compared to the value obtained with thrombin alone and expressed as a percentage (n = 6 for all conditions except chymotrypsin concentrations of 0.01, 0.5 and 1 U·ml^{-1}, where n = 5). *$P < 0.05$ (Kruskal–Wallis followed by Dunn's test). (f) Concentration–response curve of PAR1 disarming by chymotrypsin in PAR2$^{-/-}$ CMT93. The Y axis represents the percentage of the response induced by thrombin alone. The curve was generated after log transformation of the chymotrypsin concentrations, followed by a non-linear regression for normalized responses with a standard Hill slope fixed at −1. The calculated IC$_{50}$ was 0.020 U·ml^{-1} with a 95% confidence interval of [0.013; 0.030]. (g) Representative calcium response curves of Fluo-8-loaded PAR2$^{-/-}$ CMT93 cells pre-treated or not with 10-U·ml^{-1} chymotrypsin and then stimulated with the PAR1 agonist peptide TFLLR (25 μM) as described in (b). The F_{max} obtained with TFLLR after pre-incubation or not with chymotrypsin was reported on the right-hand graph (n = 5 independent experiments). ns, non-significant (Wilcoxon matched-pairs signed-rank test). Each panel represents five or more independent experiments. (h) Effect of PAR1 disarming on thrombin-induced ERK1/2 phosphorylation. PAR2$^{-/-}$ CMT93 cells were first treated with 1-U·ml^{-1} chymotrypsin or its vehicle. Two minutes later, cells were washed once in HBSS, and a second treatment was performed with 10-U·ml^{-1} thrombin or 25-μM PAR1-activating peptide (TFLLR) for 5 min. Cell lysates were analysed by Western blot using anti-phosphorylated ERK1/2 (P-ERK) antibodies and then anti-total ERK1/2 antibodies. The ratios between P-ERK and total ERK signals were quantified by densitometric analysis and represented on the right-hand panels. Each dot on the plot represents one independent experiment (n = 5 independent experiments). *$P < 0.05$ (Friedman followed by Dunn's multiple comparisons test).

3.7 | Blocking or desensitizing PAR1 does not affect PAR2 activation by chymotrypsin

We next investigated whether PAR1 disarming by chymotrypsin could influence the PAR2-dependent calcium response. To do so, we performed calcium mobilization experiments in CMT93 WT cells in the absence or presence of the PAR1 antagonist F16357, in order to block any possible PAR1-dependent signalling during the activation of PAR2. Our results showed that blocking PAR1 during chymotrypsin stimulation of CMT93 WT cells did not modify the PAR2-dependent calcium response (Figure 2d). Similarly, when we first treated HEK cells with thrombin to desensitize PAR1, we did not affect the PAR2 activation response by chymotrypsin (Figure S8). Therefore, neither PAR1 disarming nor its activation/desensitization impacts the PAR2-dependent calcium response induced by chymotrypsin. Taken together, these results suggest an absence of crosstalk between both receptors during chymotrypsin stimulation.

3.8 | Chymotrypsin triggers PAR2-dependent and PAR2-independent gene regulation

Because chymotrypsin activates PAR2, we next investigated the consequence of this signalling on gene expression using the treatment of human primary organoids. Colon-derived organoids were chronically treated with 0.5-U·ml^{-1} chymotrypsin in the absence or presence of the PAR2 antagonist I-191 (10 μM) (Figure 9a). Daily microscopic observations of organoid cultures did not reveal a significant effect of

our treatments on the development of organoids. We then analysed the impact of chymotrypsin on some key genes involved in permeability (tight junction genes such as *OCLN*, *TJP1*, *CLDN1*, *CLDN4* and *CLDN2*), immune regulation (pro-inflammatory and anti-inflammatory mediators such as *TNFA*, *CXCL8*, *IL10* and *TGFB*), cell differentiation markers (*MUC2*, *CHGA* and *SLC26A3*) and stemness/immaturity markers (*EGF* and *LGR5*) by RT-qPCR (Figure 9b). Our analysis showed that chymotrypsin up-regulates *LGR5*, *MUC2*, *TJP1*, *IL10* and *SLC26A3*, promoting epithelial barrier function and protective immunity. Among these genes, we found that *IL10* was up-regulated in a PAR2-dependent manner. In conclusion, chymotrypsin is able to signal to colonic epithelial cells by regulating some key genes involved in epithelial homeostasis in a PAR2-dependent and PAR2-independent manner.

4 | DISCUSSION

Our manuscript describes for the first time a signalling role for pancreatic chymotrypsin that we found present and active in the vicinity of the colonic epithelium. The potential intracellular signals resulting from the interaction between chymotrypsin and the IECs have never been explored so far. Our study clearly demonstrates that PAR1 and PAR2, two GPCRs expressed at the surface of IECs, are cleaved by this digestive enzyme. While the cleavage of PAR2 by chymotrypsin is able to transduce important intracellular signalling pathways, PAR1 cleavage prevents further signalling in response to thrombin, its canonical agonist (general schematic representation in Figure 10).

FIGURE 9 Chymotrypsin impacts gene expression in a PAR2-dependent and PAR2-independent manner in human 3D colon organoids. (a) Experimental protocol used for the treatment of 3D colonic organoids. Colonic crypts isolated from healthy human tissues were seeded in Matrigel and cultured in order to form organoids. At Days 4, 6 and 8, organoids were treated with 0.5-U·ml^{-1} chymotrypsin in the presence or absence of 10 μM of the PAR2 antagonist, I-191. Organoids were lysed on Day 10 for molecular analysis. (b) Gene expression profile of organoids exposed to chymotrypsin. The expression level of several genes was measured by RT-qPCR. The results are expressed as a ratio of expression (fold change) of the treated condition (0.5) compared to the control condition (0) in the absence or presence of I-191. *Hprt* was used as a housekeeping gene. Each point represents one patient (n = 6 patients for all genes, except for *IL10*, which includes n = 5). *$P < 0.05$ (Friedman test followed by Dunn's multiple comparisons test).
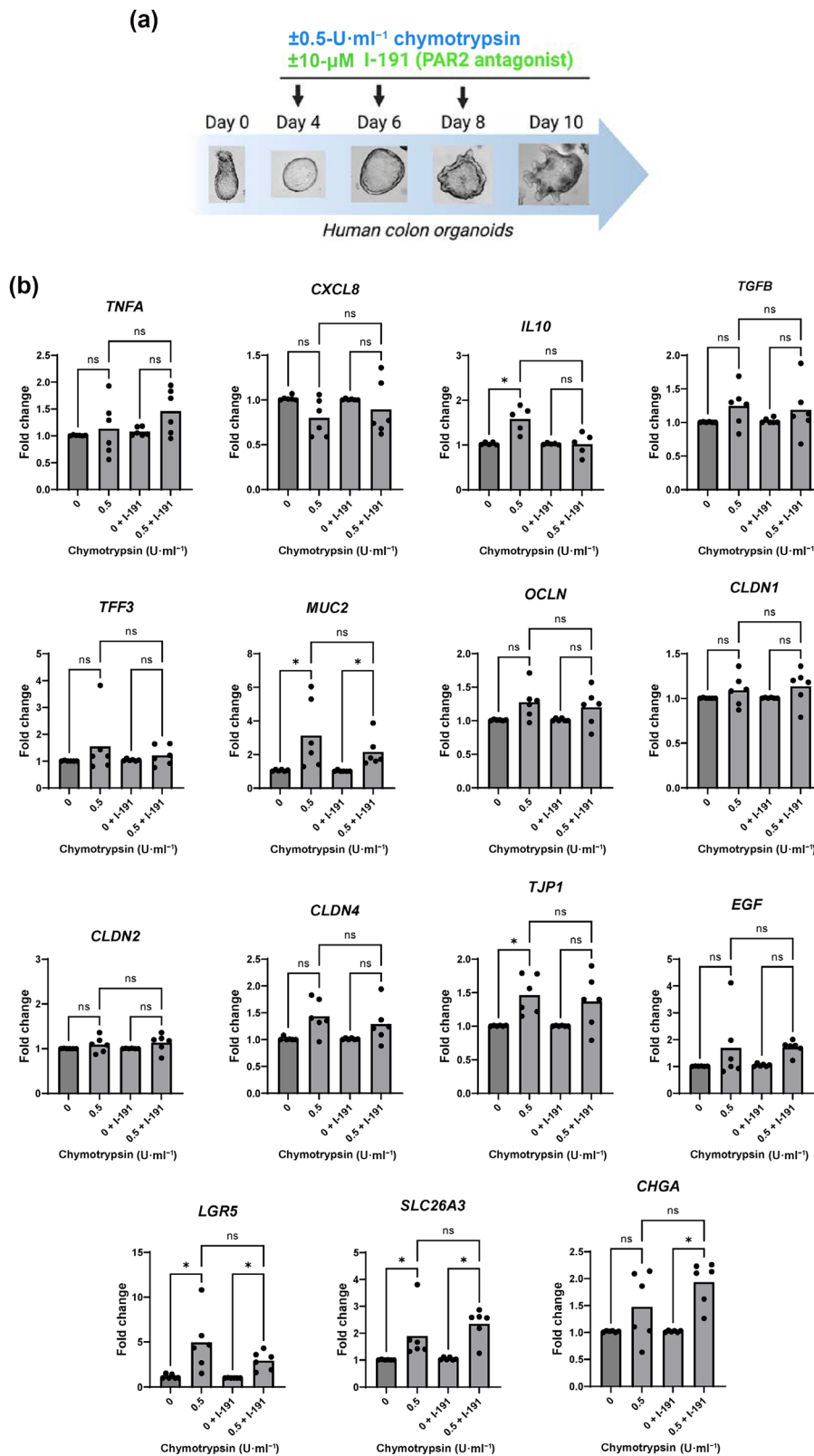
In addition to the small intestine, our data show that the apical side of the colonic epithelium is adjacent to active chymotrypsin under physiological conditions. Nevertheless, we observed a high heterogeneity in chymotrypsin activity present in faeces and mucus-containing extracts. This variability might be explained by the fact that pancreatic juice is not permanently secreted into the gut lumen but is regulated by food intake through humoral and neuronal controls (Singer & Niebergall-Roth, 2009). A similar variation was also
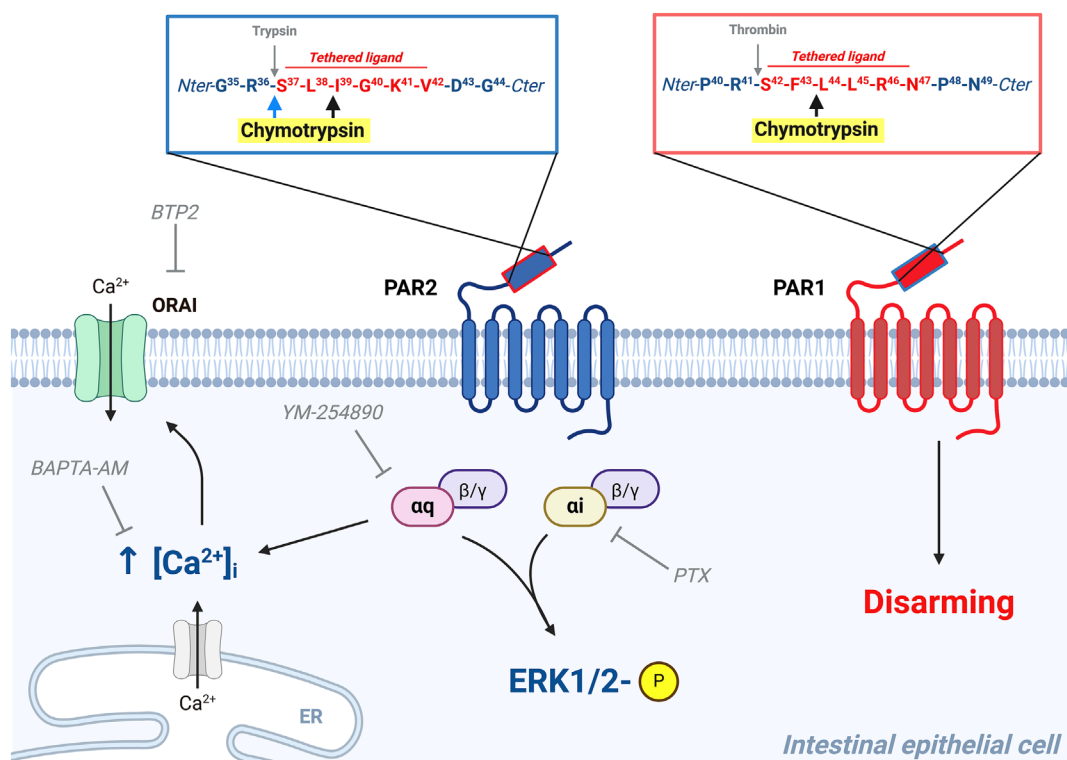
FIGURE 10 Schematic representation of chymotrypsin interactions with PAR1 and PAR2 at the surface of intestinal epithelial cells CMT93. Pancreatic chymotrypsin is able to cleave both PAR1 and PAR2. In vitro, the cleavage of PAR2 by chymotrypsin occurs at an atypical site (L^{38}/I^{39}) located within the tethered ligand sequence (dark arrow). However, in a cell context, this protease might use the PAR2 canonical R^{36}/S^{37} cleavage site to trigger calcium signalling and ERK1/2 phosphorylation (blue arrow). ERK activation is partially mediated by G_q and $G_{i/o}$ proteins, whereas calcium signalling is fully dependent on G_q. This calcium mobilization is composed of an initial ER store release followed by a long-lasting Ca^{2+} release-activated Ca^{2+} channel (CRAC) activation, enabling calcium entry from the extracellular medium. Conversely, chymotrypsin disarms PAR1 for further activation by its canonical activator thrombin by cleaving within the PAR1 tethered ligand at the F^{43}/L^{44} bond (dark arrow). Adapted from 'Activation of Protein Kinase C (PKC)', by BioRender.com (2022). Retrieved from Publication Licence NN2566RCT9.

observed in another study analysing the chymotrypsin activity content in infant stools (Remtulla et al., 1986). Accordingly, the molecular pathways that we describe in this study involving chymotrypsin and its cleaving activity on PAR1/2 are likely to operate physiologically in the gut, but in a discontinuous manner.

Our results demonstrate that chymotrypsin activates intracellular calcium signalling and ERK1/2 pathways exclusively through PAR2 in the IEC cell line CMT93. Knowing that PAR2 has been shown to exert pleiotropic functions, one can predict an array of physiological consequences that chymotrypsin could have on gut homeostasis. In vivo, the intraluminal administration of PAR2 activators has been observed to increase epithelial paracellular permeability (Cenac et al., 2002; Roka et al., 2007). In addition, publications have also reported that stimulation of PAR2 in IEC cell lines triggers electrolyte transport, chemokine or eicosanoid secretion and inhibition of cytokine-induced apoptosis (Iablokov et al., 2014; Kong et al., 1997; Tanaka et al., 2008; van der Merwe et al., 2008). Regarding chymotrypsin, one study has revealed that this enzyme triggers a decrease of ion permeability in SCBN cells, which was dependent on PKC-zeta activation but not on PAR2 (Swystun et al., 2009). Functional studies will be needed in the

future to address the role of the chymotrypsin–PAR2 axis in the context of gut epithelial cells.

From a mechanistic point of view, we found that chymotrypsin activated the ERK1/2 pathway downstream of PAR2, via $G_{i/o}$ and G_q proteins. PAR2 activation by chymotrypsin also triggered calcium signalling through the classically described G_q-dependent pathway. Interestingly, this calcium response was biphasic with an initial intracellular ER store source followed by a CRAC-dependent, long-lasting calcium influx from the extracellular medium. This calcium influx was mostly dependent on CRAC because BTP2 drastically reduced the calcium influx, without reaching full abolition. In a recent article, Zhang et al. (2020) reported that BTP2 used at 10 µM significantly inhibits Orai1 and Orai2 channels, while causing only partial Orai3 inhibition. Because CMT93 cells express all isoforms of Orai (Figure S4), the remaining calcium influx that persists could be attributed to Orai3-mediated calcium transport. In addition, we cannot exclude that Orai-independent entry of calcium might also be involved in the residual calcium influx. This biphasic profile was not observed in CMT93 cells treated with the canonical PAR2 agonist, trypsin (Figure S1), where the prompt increase in cytosolic calcium was immediately

followed by a decrease in the calcium response never increasing afterwards. This difference in the calcium profiles was even more pronounced in renal-derived cells (HEK), which we also used to explore the pharmacology of PARs (cf. Figure 6b and the trypsin response seen in Kawabata et al., 1999). This SOCE activation could be of importance knowing that this process may potentiate or prolong the effects of the primary calcium response (Targos et al., 2005).

Our data suggest that both chymotrypsin and trypsin may use the same canonical R^{36}/S^{37} cleavage site to generate calcium signalling via PAR2. Thus, the divergent calcium profiles between these enzymes are hard to explain but could be attributed either to differences in the interaction between the enzyme and PAR2 or to a concomitant action of chymotrypsin on a cell membrane target not affected by trypsin. In line with this concept, Kaiserman et al. (2022) showed that despite cleaving at the PAR2 canonical site, granzyme K (GzmK) and trypsin had opposite effects, with granzyme K (GzmK) being unable to induce any calcium signalling while inducing extracellular signal-regulated kinase (ERK) phosphorylation. This result emphasizes the complexity of proteolytic signalling mechanisms and underlines that identifying the sole PAR2 cleavage site is not sufficient to predict which downstream signalling pathways will be activated by a protease. Furthermore, our HPLC–MS analysis identified a major cleavage site for chymotrypsin on the PAR2 N-terminus at L^{38}/I^{39}. If it occurs in living cells, this cleavage does not appear to drive calcium or ERK1/2 signalling according to our results (Figure S7). However, this cleavage could represent a way to limit PAR2 activation. This hypothesis could explain the lower magnitude of the calcium response induced by chymotrypsin compared to trypsin in CMT93 cells (cf. Figures 2b and S1C). In the literature, the cleavage of PAR2 at the L^{38}/I^{39} site has been reported to induce eosinophil degranulation, via an aspartate protease activity produced by a fungus (Matsuwaki et al., 2009). Therefore, depending on the cell context, the L^{38}/I^{39} cleavage site on PAR2 may or may not exhibit functional effects.

Based on the existing PAR2 pharmacology literature, it appears that pancreatic chymotrypsin stands out from other proteases with chymotrypsin-like activity. Indeed, while the neutrophil protease cathepsin G (CatG) disarms PAR2, KLK7 was unable to activate or disarm PAR2 in KNRK cells (De Bruyn et al., 2021; Stefansson et al., 2008). Chymase, another chymotrypsin-like protease, was unable to activate PAR2 in keratinocytes (Schechter et al., 1998). Therefore, a picture that emerges from the literature is that chymotrypsin-like activities are generally either disarming or without effect towards PAR2. However, our study contradicts this concept. Importantly, Schechter et al. (1998) also found that chymotrypsin was not able to activate PAR2, a result that is opposite to ours and which highlights the importance of the cellular context.

Our transcriptional data showed that the gene expression profile of human colonic organoids was significantly impacted by chronic exposure to chymotrypsin. Among the set of genes tested, several were up-regulated by chymotrypsin, but only one demonstrated a PAR2-dependent up-regulation, IL10. This gene encodes IL-10, an anti-inflammatory cytokine that also promotes the maintenance of

intestinal epithelium barrier function (Nguyen et al., 2021). Moreover, several genes important for gut epithelial homeostasis, including MUC2, TJP1, LGR5 and SLC26A3, were also up-regulated by chymotrypsin but independently of PAR2. Altogether, these data suggest that chymotrypsin up-regulates some genes important for the maintenance of a functional epithelial barrier. However, the mechanisms and functional relevance of these transcriptional changes deserve to be investigated in further detail in the future.

Our work clearly demonstrates that, in addition to being a PAR2 activator, chymotrypsin is a very efficient PAR1-disarming protease by cleaving the receptor 2 amino acids downstream of the canonical site, at F^{43}/L^{44}. This makes thrombin unable to signal via PAR1 anymore. Our study is in agreement with previous work, which showed that a synthetic peptide corresponding to the PAR1 N-terminal region 38–60 was cleaved at the same F^{43}/L^{44} site by chymotrypsin (Parry et al., 1996). However, the functional outcome of such a cleavage occurring on the whole receptor expressed in living cells has not been evaluated. The disarming of calcium signals that we report here also provides a functional explanation to pioneering experiments in the 1980s, which showed that platelets previously exposed to pancreatic chymotrypsin exhibited delayed thrombin-induced aggregation (Tam et al., 1980). Previous studies reported that cathepsin G (CatG) and chymase also had the ability to disarm PAR1 (De Bruyn et al., 2021; Molino et al., 1995; Renesto et al., 1997; Schechter et al., 1998). Therefore, a PAR1 disarming effect appears to be a common characteristic of chymotrypsin-like proteases.

Interestingly, in our experiments, the IC_{50} for PAR1 disarming by chymotrypsin was very low, that is, 0.02 U·ml^{-1} (corresponding to 12 nM), a concentration at which no effect on PAR2 is observed. Similarly, Parry et al. (1996) concluded that, despite a lower cleavage efficiency, the affinity of chymotrypsin for PAR1 was equivalent to that of thrombin, making PAR1 a very good chymotrypsin substrate. These observations suggest that, under physiological conditions, pancreatic chymotrypsin present in the lumen could disarm PAR1 well before activating PAR2. The physiological effect of this disarming remains to be elucidated, but because thrombin has been shown to be secreted in the gut lumen by IECs (Motta et al., 2019; Motta, Deraison, et al., 2021; Motta, Palese, et al., 2021), PAR1 activation and disarming actions are relevant at the apical side of the epithelium. Notably, our team has shown that colonic exposure to a high dose of thrombin causes mucosal damage in a PAR1-dependent manner (Motta, Palese, et al., 2021). Precisely, it was shown that PAR1 is involved in various parameters of the inflammatory response such as a higher epithelial apoptosis, a higher permeability and a higher bacterial translocation. The presence of chymotrypsin close to the colonic epithelium could therefore prevent the development of colitis induced by thrombin-dependent activation of PAR1. In human organoids, PAR1 cleavage by thrombin has been associated with increased epithelial cell maturation and apoptosis (Sebert et al., 2018). In contrast, Darmoul et al. (2003) linked PAR1 expression to a cancerous context. The same group reported that activation of PAR1 by thrombin or its agonist peptide TFLLR drives proliferation of HT29 cells (Darmoul et al., 2004). Chymotrypsin, by disarming PAR1, could therefore have anti-apoptotic or

anti-proliferative effects depending on the context (primary vs. cancerous IECs). In summary, our results suggest that chymotrypsin could be a major regulator of PAR1 and PAR2 activity at the intestinal epithelium surface.

5 | CONCLUSION

Taken together, our results clearly define chymotrypsin as a luminal protease of the gut that neighbours the colonic epithelium, where PARs are expressed. We show that, in IECs, chymotrypsin cleaves the extracellular domains of PAR2 and PAR1 and thereby transduces or prevents intracellular signals, respectively. Our transcriptional study on human primary colonic organoids revealed that chymotrypsin triggers the expression of epithelial protection-associated genes, and one of them, IL-10, is specifically induced via PAR2 activation. Our data define a new potential role of luminal chymotrypsin as a regulator of gut epithelial signalling. Future work is thus warranted to determine the role of chymotrypsin signalling in intestinal inflammation and cancer.

AUTHOR CONTRIBUTIONS

Simon Guignard: Conceptualization; formal analysis; funding acquisition; investigation; validation; visualization; writing—original draft. **Mahmoud Saifeddine:** Formal analysis; investigation. **Koichiro Mihara:** Formal analysis; investigation. **Majid Motahhary:** Formal analysis; investigation. **Magali Savignac:** Resources; writing—review and editing. **Laura Guiraud:** Formal analysis; investigation. **David Sagnat:** Formal analysis; investigation. **Mireille Sebbag:** Investigation; resources; writing—review and editing. **Sokchea Khou:** Formal analysis; investigation. **Corinne Rolland:** Formal analysis; investigation. **Anissa Edir:** Data curation; formal analysis; investigation; methodology. **Barbara Bournet:** Resources. **Louis Buscail:** Resources. **Etienne Buscail:** Resources. **Laurent Alric:** Resources. **Caroline Camare:** Resources. **Mouna Ambli:** Formal analysis; investigation. **Nathalie Vergnolle:** Conceptualization; funding acquisition; supervision; writing—review and editing. **Morley D. Hollenberg:** Funding acquisition; supervision; writing—original draft; writing—review and editing. **Céline Deraison:** Conceptualization; supervision; writing—review and editing. **Chrystelle Bonnart:** Conceptualization; formal analysis; funding acquisition; investigation; supervision; validation; visualization; writing—original draft.

CONFLICT OF INTEREST STATEMENT

The authors declare they have no actual or potential competing financial interests related to the work presented here.

DATA AVAILABILITY STATEMENT

The data supporting the findings of this study are available upon request from the corresponding author.

DECLARATION OF TRANSPARENCY AND SCIENTIFIC RIGOUR

This Declaration acknowledges that this paper adheres to the principles for transparent reporting and scientific rigour of preclinical research as stated in the *BJP* guidelines for Design & Analysis, Immunoblotting and Immunochemistry, and Animal Experimentation and as recommended by funding agencies, publishers and other organizations engaged with supporting research.

ORCID

Nathalie Vergnolle https://orcid.org/0000-0003-1825-6015
Morley D. Hollenberg https://orcid.org/0000-0003-4070-8786
Céline Deraison https://orcid.org/0000-0002-9013-4592
Chrystelle Bonnart https://orcid.org/0000-0002-3875-492X

REFERENCES

Adams, M. N., Ramachandran, R., Yau, M. K., Suen, J. Y., Fairlie, D. P., Hollenberg, M. D., & Hooper, J. D. (2011). Structure, function and pathophysiology of protease activated receptors. *Pharmacology & Therapeutics*, *130*, 248–282. https://doi.org/10.1016/j.pharmthera.2011.01.003

Alexander, S. P. H., Christopoulos, A., Davenport, A. P., Kelly, E., Mathie, A. A., Peters, J. A., Veale, E. L., Armstrong, J. F., Faccenda, E., Harding, S. D., Davies, J. A., Abbracchio, M. P., Abraham, G., Agoulnik, A., Alexander, W., Al-Hosaini, K., Bäck, M., Baker, J. G., Barnes, N. M., ... Ye, R. D. (2023). The Concise Guide to PHARMACOLOGY 2023/24: G protein-coupled receptors. *British Journal of Pharmacology*, *180*, S23–S144. https://doi.org/10.1111/bph.16177

Alexander, S. P. H., Fabbro, D., Kelly, E., Mathie, A. A., Peters, J. A., Veale, E. L., Armstrong, J. F., Faccenda, E., Harding, S. D., Davies, J. A., Annett, S., Boison, D., Burns, K. E., Dessauer, C., Gertsch, J., Helsby, N. A., Izzo, A. A., Ostrom, R., Papapetropoulos, A., ... Wong, S. S. (2023). The Concise Guide to PHARMACOLOGY 2023/24: Enzymes. *British Journal of Pharmacology*, *180*, S289–S373. https://doi.org/10.1111/bph.16181

Alexander, S. P. H., Mathie, A. A., Peters, J. A., Veale, E. L., Striessnig, J., Kelly, E., Armstrong, J. F., Faccenda, E., Harding, S. D., Davies, J. A., Aldrich, R. W., Attali, B., Baggetta, A. M., Becirovic, E., Biel, M., Bill, R. M., Caceres, A. I., Catterall, W. A., Conner, A. C., ... Zhu, M. (2023). The Concise Guide to PHARMACOLOGY 2023/24: Ion channels. *British Journal of Pharmacology*, *180*, S145–S222. https://doi.org/10.1111/bph.16181

Alexander, S. P. H., Roberts, R. E., Broughton, B. R. S., Sobey, C. G., George, C. H., Stanford, S. C., Cirino, G., Docherty, J. R., Giembycz, M. A., Hoyer, D., Insel, P. A., Izzo, A. A., Ji, Y., MacEwan, D. J., Mangum, J., Wonnacott, S., ... Ahluwalia, A. (2018). Goals and practicalities of immunoblotting and immunohistochemistry: A guide for submission to the *British Journal of Pharmacology*. *British*

Journal of Pharmacology, *175*, 407–411. https://doi.org/10.1111/bph. 14112

Bohm, S. K., Kong, W., Bromme, D., Smeekens, S. P., Anderson, D. C., Connolly, A., Kahn, M., Nelken, N. A., Coughlin, S. R., Payan, D. G., & Bunnett, N. W. (1996). Molecular cloning, expression and potential functions of the human proteinase-activated receptor-2. *The Biochemical Journal*, *314*(Pt 3), 1009–1016. https://doi.org/10.1042/bj3141009

Borgstrom, B., Dahlqvist, A., Lundh, G., & Sjovall, J. (1957). Studies of intestinal digestion and absorption in the human. *The Journal of Clinical Investigation*, *36*, 1521–1536. https://doi.org/10.1172/JCI103549

Buresi, M. C., Schleihauf, E., Vergnolle, N., Buret, A., Wallace, J. L., Hollenberg, M. D., & MacNaughton, W. K. (2001). Protease-activated receptor-1 stimulates Ca^{2+}-dependent $Cl^−$ secretion in human intestinal epithelial cells. *American Journal of Physiology. Gastrointestinal and Liver Physiology*, *281*, G323–G332. https://doi.org/10.1152/ajpgi. 2001.281.2.G323

Caminero, A., McCarville, J. L., Galipeau, H. J., Deraison, C., Bernier, S. P., Constante, M., Rolland, C., Meisel, M., Murray, J. A., Yu, X. B., Alaedini, A., Coombes, B. K., Bercik, P., Southward, C. M., Ruf, W., Jabri, B., Chirdo, F. G., Casqueiro, J., Surette, M. G., ... Verdu, E. F. (2019). Duodenal bacterial proteolytic activity determines sensitivity to dietary antigen through protease-activated receptor-2. *Nature Communications*, *10*, 1198. https://doi.org/10.1038/s41467-019-09037-9

Canivet, C., Gourgou-Bourgade, S., Napoleon, B., Palazzo, L., Flori, N., Guibert, P., Piessen, G., Farges-Bancel, D., Seitz, J. F., Assenat, E., Vendrely, V., Truant, S., Vanbiervliet, G., Berthelemy, P., Garcia, S., Gomez-Brouchet, A., Buscail, L., Bournet, B., & Bacap Consortium. (2018). A prospective clinical and biological database for pancreatic adenocarcinoma: The BACAP cohort. *BMC Cancer*, *18*, 986. https://doi.org/10.1186/s12885-018-4906-4

Cenac, N., Coelho, A. M., Nguyen, C., Compton, S., Andrade-Gordon, P., MacNaughton, W. K., Wallace, J. L., Hollenberg, M. D., Bunnett, N. W., Garcia-Villar, R., Bueno, L., & Vergnolle, N. (2002). Induction of intestinal inflammation in mouse by activation of proteinase-activated receptor-2. *The American Journal of Pathology*, *161*, 1903–1915. https://doi.org/10.1016/S0002-9440(10)64466-5

Chin, A. C., Vergnolle, N., MacNaughton, W. K., Wallace, J. L., Hollenberg, M. D., & Buret, A. G. (2003). Proteinase-activated receptor 1 activation induces epithelial apoptosis and increases intestinal permeability. *Proceedings of the National Academy of Sciences of the United States of America*, *100*, 11104–11109. https://doi.org/10.1073/pnas.1831452100

Cuffe, J. E., Bertog, M., Velazquez-Rocha, S., Dery, O., Bunnett, N., & Korbmacher, C. (2002). Basolateral PAR-2 receptors mediate KCl secretion and inhibition of Na^+ absorption in the mouse distal colon. *The Journal of Physiology*, *539*, 209–222. https://doi.org/10.1113/jphysiol.2001.013159

Curtis, M. J., Alexander, S. P. H., Cirino, G., George, C. H., Kendall, D. A., Insel, P. A., Izzo, A. A., Ji, Y., Panettieri, R. A., Patel, H. H., Sobey, C. G., Stanford, S. C., Stanley, P., Stefanska, B., Stephens, G. J., Teixeira, M. M., Vergnolle, N., & Ahluwalia, A. (2022). Planning experiments: Updated guidance on experimental design and analysis and their reporting III. *British Journal of Pharmacology*, *179*(15), 3907–3913. https://doi.org/10.1111/bph.15868

D'Andrea, M. R., Derian, C. K., Leturcq, D., Baker, S. M., Brunmark, A., Ling, P., Darrow, A. L., Santulli, R. J., Brass, L. F., & Andrade-Gordon, P. (1998). Characterization of protease-activated receptor-2 immunoreactivity in normal human tissues. *The Journal of Histochemistry and Cytochemistry*, *46*, 157–164. https://doi.org/10.1177/002215549 804600204

Darmoul, D., Gratio, V., Devaud, H., Lehy, T., & Laburthe, M. (2003). Aberrant expression and activation of the thrombin receptor protease-activated receptor-1 induces cell proliferation and motility in human colon cancer cells. *The American Journal of Pathology*, *162*, 1503–1513. https://doi.org/10.1016/S0002-9440(10)64283-6

Darmoul, D., Gratio, V., Devaud, H., Peiretti, F., & Laburthe, M. (2004). Activation of proteinase-activated receptor 1 promotes human colon cancer cell proliferation through epidermal growth factor receptor transactivation. *Molecular Cancer Research*, *2*, 514–522. https://doi.org/10.1158/1541-7786.514.2.9

De Bruyn, M., Ceuleers, H., Hanning, N., Berg, M., De Man, J. G., Hulpiau, P., Hermans, C., Stenman, U. H., Koistinen, H., Lambeir, A. M., De Winter, B. Y., & De Meester, I. (2021). Proteolytic cleavage of bioactive peptides and protease-activated receptors in acute and post-colitis. *International Journal of Molecular Sciences*, *22*, 10711. https://doi.org/10.3390/ijms221910711

Dulon, S., Cande, C., Bunnett, N. W., Hollenberg, M. D., Chignard, M., & Pidard, D. (2003). Proteinase-activated receptor-2 and human lung epithelial cells: Disarming by neutrophil serine proteinases. *American Journal of Respiratory Cell and Molecular Biology*, *28*, 339–346. https://doi.org/10.1165/rcmb.4908

Goldberg, D. M., Campbell, R., & Roy, A. D. (1968). Binding of trypsin and chymotrypsin by human intestinal mucosa. *Biochimica et Biophysica Acta*, *167*, 613–615. https://doi.org/10.1016/0005-2744(68)90053-3

Goldberg, D. M., Campbell, R., & Roy, A. D. (1969). Fate of trypsin and chymotrypsin in the human small intestine. *Gut*, *10*, 477–483.

Hollenberg, M. D., Mihara, K., Polley, D., Suen, J. Y., Han, A., Fairlie, D. P., & Ramachandran, R. (2014). Biased signalling and proteinase-activated receptors (PARs): Targeting inflammatory disease. *British Journal of Pharmacology*, *171*, 1180–1194. https://doi.org/10.1111/bph.12544

Holzhausen, M., Spolidorio, L. C., Ellen, R. P., Jobin, M. C., Steinhoff, M., Andrade-Gordon, P., & Vergnolle, N. (2006). Protease-activated receptor-2 activation: A major role in the pathogenesis of *Porphyromonas gingivalis* infection. *The American Journal of Pathology*, *168*, 1189–1199. https://doi.org/10.2353/ajpath.2006.050658

Iablokov, V., Hirota, C. L., Peplowski, M. A., Ramachandran, R., Mihara, K., Hollenberg, M. D., & MacNaughton, W. K. (2014). Proteinase-activated receptor 2 (PAR2) decreases apoptosis in colonic epithelial cells. *The Journal of Biological Chemistry*, *289*, 34366–34377. https://doi.org/10.1074/jbc.M114.610485

Kaiserman, D., Zhao, P., Rowe, C. L., Leong, A., Barlow, N., Joeckel, L. T., Hitchen, C., Stewart, S. E., Hollenberg, M. D., Bunnett, N., Suhrbier, A., & Bird, P. I. (2022). Granzyme K initiates IL-6 and IL-8 release from epithelial cells by activating protease-activated receptor 2. *PLoS ONE*, *17*, e0270584. https://doi.org/10.1371/journal.pone.0270584

Kawabata, A., Saifeddine, M., Al-Ani, B., Leblond, L., & Hollenberg, M. D. (1999). Evaluation of proteinase-activated receptor-1 (PAR1) agonists and antagonists using a cultured cell receptor desensitization assay: Activation of PAR2 by PAR1-targeted ligands. *The Journal of Pharmacology and Experimental Therapeutics*, *288*, 358–370.

Kong, W., McConalogue, K., Khitin, L. M., Hollenberg, M. D., Payan, D. G., Bohm, S. K., & Bunnett, N. W. (1997). Luminal trypsin may regulate enterocytes through proteinase-activated receptor 2. *Proceedings of the National Academy of Sciences of the United States of America*, *94*, 8884–8889. https://doi.org/10.1073/pnas.94.16.8884

Lau, C., Lytle, C., Straus, D. S., & DeFea, K. A. (2011). Apical and basolateral pools of proteinase-activated receptor-2 direct distinct signaling events in the intestinal epithelium. *American Journal of Physiology. Cell Physiology*, *300*, C113–C123. https://doi.org/10.1152/ajpcell.00162. 2010

Lilley, E., Stanford, S. C., Kendall, D. E., Alexander, S. P. H., Cirino, G., Docherty, J. R., George, C. H., Insel, P. A., Izzo, A. A., Ji, Y., Panettieri, R. A., Sobey, C. G., Stefanska, B., Stephens, G., Teixeira, M., & Ahluwalia, A. (2020). ARRIVE 2.0 and the British Journal of Pharmacology: Updated guidance for 2020. *British Journal of Pharmacology*, *177*, 3611–3616. https://doi.org/10.1111/bph.15178

Livak, K. J., & Schmittgen, T. D. (2001). Analysis of relative gene expression data using real-time quantitative PCR and the $2^{-\Delta\Delta CT}$ method. *Methods*, *25*, 402–408. https://doi.org/10.1006/meth.2001.1262

Matsuwaki, Y., Wada, K., White, T. A., Benson, L. M., Charlesworth, M. C., Checkel, J. L., Inoue, Y., Hotta, K., Ponikau, J. U., Lawrence, C. B., & Kita, H. (2009). Recognition of fungal protease activities induces cellular activation and eosinophil-derived neurotoxin release in human eosinophils. *Journal of Immunology*, *183*, 6708–6716. https://doi.org/10.4049/jimmunol.0901220

Mihara, K., Ramachandran, R., Renaux, B., Saifeddine, M., & Hollenberg, M. D. (2013). Neutrophil elastase and proteinase-3 trigger G protein-biased signaling through proteinase-activated receptor-1 (PAR1). *The Journal of Biological Chemistry*, *288*, 32979–32990. https://doi.org/10.1074/jbc.M113.483123

Mihara, K., Ramachandran, R., Saifeddine, M., Hansen, K. K., Renaux, B., Polley, D., Gibson, S., Vanderboor, C., & Hollenberg, M. D. (2016). Thrombin-mediated direct activation of proteinase-activated receptor-2: Another target for thrombin signaling. *Molecular Pharmacology*, *89*, 606–614. https://doi.org/10.1124/mol.115.102723

Molino, M., Blanchard, N., Belmonte, E., Tarver, A. P., Abrams, C., Hoxie, J. A., Cerletti, C., & Brass, L. F. (1995). Proteolysis of the human platelet and endothelial cell thrombin receptor by neutrophil-derived cathepsin G. *The Journal of Biological Chemistry*, *270*, 11168–11175. https://doi.org/10.1074/jbc.270.19.11168

Motta, J. P., Denadai-Souza, A., Sagnat, D., Guiraud, L., Edir, A., Bonnart, C., Sebbag, M., Rousset, P., Lapeyre, A., Seguy, C., Mathurine-Thomas, N., Galipeau, H. J., Bonnet, D., Alric, L., Buret, A. G., Wallace, J. L., Dufour, A., Verdu, E. F., Hollenberg, M. D., … Vergnolle, N. (2019). Active thrombin produced by the intestinal epithelium controls mucosal biofilms. *Nature Communications*, *10*, 3224. https://doi.org/10.1038/s41467-019-11140-w

Motta, J. P., Deraison, C., Le Grand, S., Le Grand, B., & Vergnolle, N. (2021). PAR-1 antagonism to promote gut mucosa healing in Crohn's disease patients: A new avenue for CVT120165. *Inflammatory Bowel Diseases*, *27*, S33–S37. https://doi.org/10.1093/ibd/izab244

Motta, J. P., Palese, S., Giorgio, C., Chapman, K., Denadai-Souza, A., Rousset, P., Sagnat, D., Guiraud, L., Edir, A., Seguy, C., Alric, L., Bonnet, D., Bournet, B., Buscail, L., Gilletta, C., Buret, A. G., Wallace, J. L., Hollenberg, M. D., Oswald, E., … Vergnolle, N. (2021). Increased mucosal thrombin is associated with Crohn's disease and causes inflammatory damage through protease-activated receptors activation. *Journal of Crohn's & Colitis*, *15*, 787–799. https://doi.org/10.1093/ecco-jcc/jjaa229

Nasri, I., Bonnet, D., Zwarycz, B., d'Aldebert, E., Khou, S., Mezghani-Jarraya, R., Quaranta, M., Rolland, C., Bonnart, C., Mas, E., Ferrand, A., Cenac, N., Magness, S., Van Landeghem, L., Vergnolle, N., & Racaud-Sultan, C. (2016). PAR$_2$-dependent activation of GSK3β regulates the survival of colon stem/progenitor cells. *American Journal of Physiology. Gastrointestinal and Liver Physiology*, *311*, G221–G236. https://doi.org/10.1152/ajpgi.00328.2015

Nguyen, C., Coelho, A. M., Grady, E., Compton, S. J., Wallace, J. L., Hollenberg, M. D., Cenac, N., Garcia-Villar, R., Bueno, L., Steinhoff, M., Bunnett, N. W., & Vergnolle, N. (2003). Colitis induced by proteinase-activated receptor-2 agonists is mediated by a neurogenic mechanism. *Canadian Journal of Physiology and Pharmacology*, *81*, 920–927. https://doi.org/10.1139/y03-080

Nguyen, H. D., Aljamaei, H. M., & Stadnyk, A. W. (2021). The production and function of endogenous interleukin-10 in intestinal epithelial cells and gut homeostasis. *Cellular and Molecular Gastroenterology and Hepatology*, *12*, 1343–1352. https://doi.org/10.1016/j.jcmgh.2021.07.005

Nystedt, S., Emilsson, K., Larsson, A. K., Strombeck, B., & Sundelin, J. (1995). Molecular cloning and functional expression of the gene encoding the human proteinase-activated receptor 2. *European Journal of Biochemistry*, *232*, 84–89. https://doi.org/10.1111/j.1432-1033.1995.tb20784.x

Nystedt, S., Emilsson, K., Wahlestedt, C., & Sundelin, J. (1994). Molecular cloning of a potential proteinase activated receptor. *Proceedings of the National Academy of Sciences of the United States of America*, *91*, 9208–9212. https://doi.org/10.1073/pnas.91.20.9208

Nystedt, S., Larsson, A. K., Aberg, H., & Sundelin, J. (1995). The mouse proteinase-activated receptor-2 cDNA and gene. Molecular cloning and functional expression. *The Journal of Biological Chemistry*, *270*, 5950–5955.

Oikonomopoulou, K., Hansen, K. K., Saifeddine, M., Tea, I., Blaber, M., Blaber, S. I., Scarisbrick, I., Andrade-Gordon, P., Cottrell, G. S., Bunnett, N. W., Diamandis, E. P., & Hollenberg, M. D. (2006). Proteinase-activated receptors, targets for kallikrein signaling. *The Journal of Biological Chemistry*, *281*, 32095–32112. https://doi.org/10.1074/jbc.M513138200

Pandol, S. J. (2010). The exocrine pancreas. *Morgan & Claypool Life Sciences*. https://doi.org/10.4199/C00026ED1V01Y201102ISP014

Parry, M. A., Myles, T., Tschopp, J., & Stone, S. R. (1996). Cleavage of the thrombin receptor: Identification of potential activators and inactivators. *The Biochemical Journal*, *320*(Pt 1), 335–341. https://doi.org/10.1042/bj3200335

Peach, C. J., Edgington-Mitchell, L. E., Bunnett, N. W., & Schmidt, B. L. (2023). Protease-activated receptors in health and disease. *Physiological Reviews*, *103*, 717–785. https://doi.org/10.1152/physrev.00044.2021

Percie du Sert, N., Hurst, V., Ahluwalia, A., Alam, S., Avey, M. T., Baker, M., Browne, W. J., Clark, A., Cuthill, I. C., Dirnagl, U., Emerson, M., Garner, P., Holgate, S. T., Howells, D. W., Karp, N. A., Lazic, S. E., Lidster, K., MacCallum, C. J., Macleod, M., … Würbel, H. (2020). The ARRIVE guidelines 2.0: Updated guidelines for reporting animal research. *PLoS Biology*, *18*(7), e3000410. https://doi.org/10.1371/journal.pbio.3000410

Ramachandran, R., Altier, C., Oikonomopoulou, K., & Hollenberg, M. D. (2016). Proteinases, their extracellular targets, and inflammatory signaling. *Pharmacological Reviews*, *68*, 1110–1142. https://doi.org/10.1124/pr.115.010991

Ramachandran, R., Mihara, K., Chung, H., Renaux, B., Lau, C. S., Muruve, D. A., DeFea, K. A., Bouvier, M., & Hollenberg, M. D. (2011). Neutrophil elastase acts as a biased agonist for proteinase-activated receptor-2 (PAR2). *The Journal of Biological Chemistry*, *286*, 24638–24648. https://doi.org/10.1074/jbc.M110.201988

Ramachandran, R., Mihara, K., Mathur, M., Rochdi, M. D., Bouvier, M., Defea, K., & Hollenberg, M. D. (2009). Agonist-biased signaling via proteinase activated receptor-2: Differential activation of calcium and mitogen-activated protein kinase pathways. *Molecular Pharmacology*, *76*, 791–801. https://doi.org/10.1124/mol.109.055509

Ramachandran, R., Noorbakhsh, F., Defea, K., & Hollenberg, M. D. (2012). Targeting proteinase-activated receptors: Therapeutic potential and challenges. *Nature Reviews. Drug Discovery*, *11*, 69–86. https://doi.org/10.1038/nrd3615

Reinhardt, C., Bergentall, M., Greiner, T. U., Schaffner, F., Ostergren-Lunden, G., Petersen, L. C., Ruf, W., & Backhed, F. (2012). Tissue factor and PAR1 promote microbiota-induced intestinal vascular remodelling. *Nature*, *483*, 627–631. https://doi.org/10.1038/nature10893

Remtulla, M. A., Durie, P. R., & Goldberg, D. M. (1986). Stool chymotrypsin activity measured by a spectrophotometric procedure to identify pancreatic disease in infants. *Clinical Biochemistry*, *19*, 341–347. https://doi.org/10.1016/S0009-9120(86)80007-8

Renesto, P., Si-Tahar, M., Moniatte, M., Balloy, V., Van Dorsselaer, A., Pidard, D., & Chignard, M. (1997). Specific inhibition of thrombin-induced cell activation by the neutrophil proteinases elastase, cathepsin G, and proteinase 3: Evidence for distinct cleavage sites within the aminoterminal domain of the thrombin receptor. *Blood*, *89*, 1944–1953. https://doi.org/10.1182/blood.V89.6.1944

Roka, R., Demaude, J., Cenac, N., Ferrier, L., Salvador-Cartier, C., Garcia-Villar, R., Fioramonti, J., & Bueno, L. (2007). Colonic luminal proteases

activate colonocyte proteinase-activated receptor-2 and regulate paracellular permeability in mice. *Neurogastroenterology and Motility*, *19*, 57–65. https://doi.org/10.1111/j.1365-2982.2006.00851.x

Schechter, N. M., Brass, L. F., Lavker, R. M., & Jensen, P. J. (1998). Reaction of mast cell proteases tryptase and chymase with protease activated receptors (PARs) on keratinocytes and fibroblasts. *Journal of Cellular Physiology*, *176*, 365–373. https://doi.org/10.1002/(SICI)1097-4652(199808)176:2<365::AID-JCP15>3.0.CO;2-2

Sebert, M., Denadai-Souza, A., Quaranta, M., Racaud-Sultan, C., Chabot, S., Lluel, P., Monjotin, N., Alric, L., Portier, G., Kirzin, S., Bonnet, D., Ferrand, A., & Vergnolle, N. (2018). Thrombin modifies growth, proliferation and apoptosis of human colon organoids: A protease-activated receptor 1- and protease-activated receptor 4-dependent mechanism. *British Journal of Pharmacology*, *175*, 3656–3668. https://doi.org/10.1111/bph.14430

Sebert, M., Sola-Tapias, N., Mas, E., Barreau, F., & Ferrand, A. (2019). Protease-activated receptors in the intestine: Focus on inflammation and cancer. *Front Endocrinol (Lausanne)*, *10*, 717. https://doi.org/10.3389/fendo.2019.00717

Singer, M. V., & Niebergall-Roth, E. (2009). Secretion from acinar cells of the exocrine pancreas: Role of enteropancreatic reflexes and cholecystokinin. *Cell Biology International*, *33*, 1–9. https://doi.org/10.1016/j.cellbi.2008.09.008

Smith, J. S., Ediss, I., Mullinger, M. A., & Bogoch, A. (1971). Fecal chymotrypsin and trypsin determinations. *Canadian Medical Association Journal*, *104*, 691-4 passim.

Stefansson, K., Brattsand, M., Roosterman, D., Kempkes, C., Bocheva, G., Steinhoff, M., & Egelrud, T. (2008). Activation of proteinase-activated receptor-2 by human kallikrein-related peptidases. *The Journal of Investigative Dermatology*, *128*, 18–25. https://doi.org/10.1038/sj.jid.5700965

Swystun, V. A., Renaux, B., Moreau, F., Wen, S., Peplowski, M. A., Hollenberg, M. D., & MacNaughton, W. K. (2009). Serine proteases decrease intestinal epithelial ion permeability by activation of protein kinase Cζ. *American Journal of Physiology. Gastrointestinal and Liver Physiology*, *297*, G60–G70. https://doi.org/10.1152/ajpgi.00096.2009

Tam, S. W., Fenton, J. W. 2nd, & Detwiler, T. C. (1980). Platelet thrombin receptors. Binding of alpha-thrombin is coupled to signal generation by a chymotrypsin-sensitive mechanism. *The Journal of Biological Chemistry*, *255*, 6626–6632. https://doi.org/10.1016/S0021-9258(18)43615-0

Tanaka, Y., Sekiguchi, F., Hong, H., & Kawabata, A. (2008). PAR2 triggers IL-8 release via MEK/ERK and PI3-kinase/Akt pathways in GI epithelial cells. *Biochemical and Biophysical Research Communications*, *377*, 622–626. https://doi.org/10.1016/j.bbrc.2008.10.018

Targos, B., Baranska, J., & Pomorski, P. (2005). Store-operated calcium entry in physiology and pathology of mammalian cells. *Acta Biochimica Polonica*, *52*, 397–409. https://doi.org/10.18388/abp.2005_3452

van der Merwe, J. Q., Hollenberg, M. D., & MacNaughton, W. K. (2008). EGF receptor transactivation and MAP kinase mediate proteinase-activated receptor-2-induced chloride secretion in intestinal epithelial cells. *American Journal of Physiology. Gastrointestinal and Liver Physiology*, *294*, G441–G451. https://doi.org/10.1152/ajpgi.00303.2007

Vergnolle, N. (2005). Clinical relevance of proteinase activated receptors (pars) in the gut. *Gut*, *54*, 867–874. https://doi.org/10.1136/gut.2004.048876

Vergnolle, N. (2016). Protease inhibition as new therapeutic strategy for GI diseases. *Gut*, *65*, 1215–1224. https://doi.org/10.1136/gutjnl-2015-309147

Wang, H., Ubl, J. J., Stricker, R., & Reiser, G. (2002). Thrombin (PAR-1)-induced proliferation in astrocytes via MAPK involves multiple signaling pathways. *American Journal of Physiology. Cell Physiology*, *283*, C1351–C1364. https://doi.org/10.1152/ajpcell.00001.2002

Zhang, X., Xin, P., Yoast, R. E., Emrich, S. M., Johnson, M. T., Pathak, T., Benson, J. C., Azimi, I., Gill, D. L., Monteith, G. R., & Trebak, M. (2020). Distinct pharmacological profiles of ORAI1, ORAI2, and ORAI3 channels. *Cell Calcium*, *91*, 102281. https://doi.org/10.1016/j.ceca.2020.102281

SUPPORTING INFORMATION

Additional supporting information can be found online in the Supporting Information section at the end of this article.